REPUBLIC OF TÜRKİYE

ALTINBAŞ UNIVERSITY

Institute of Graduate Studies

Electrical and Computer Engineering

BLACK WIDOW OPTIMIZATION ALGORITHM COUPLED WITH AES CRYPTO FOR MULTILEVEL IMAGE THRESHOLDING WITH IMPROVED OTSU THRESHOLDING

Anfal AL-RAHLAWEE

Doctor of Philosophy

Supervisor

Prof. Dr.Oğuz BAYAT

Istanbul, 2023

BLACK WIDOW OPTIMIZATION ALGORITHM COUPLED WITH AES CRYPTO FOR MULTILEVEL IMAGE THRESHOLDING WITH IMPROVED OTSU THRESHOLDING

Anfal AL-RAHLAWEE

Electrical and Computer Engineering

Doctor of Philosophy

ALTINBAŞ UNIVERSITY

2023

The dissertation titled "BLACK WIDOW OPTIMIZATION ALGORITHM COUPLED WITH AES CRYPTO FOR MULTILEVEL IMAGE THRESHOLDING WITH IMPROVED OTSU THRESHOLDING" prepared by Anfal Thaer Hussein and submitted on 01-03-2023 has been **accepted unanimously** for the degree of Ph.D in Electrical and Computer Engineering

Academic Title – First and Last Name of the Co-Supervisor	Academic Title – First and Last Name of the Supervisor

Thesis Defense Committee Members:

Prof. Dr. Oğuz BAYAT	Department, University	_____
Asst. Prof. Dr. Muhammad ILYAS	Department, University	_____
Asst. Prof. Dr. Abdullahi Abdu IBRAHIM	Department, University	_____
Asst. Prof. Dr. Çağatay AYDIN	Department, University	_____
Asst. Prof. Dr. Adil Deniz DURU	Department, University	_____

I hereby declare that this thesis/dissertation meets all format and submission requirements of a …… (Master's/PhD) thesis/dissertation.

Submission date of the thesis to Institute of Graduate Studies: ___/___/___

I hereby declare that all information/data presented in this graduation project has been obtained in full accordance with academic rules and ethical conduct. I also declare all unoriginal materials and conclusions have been cited in the text and all references mentioned in the Reference List have been cited in the text, and vice versa as required by the abovementioned rules and conduct.

Anfal AL-RAHLAWEE

Signature

DEDICATION

All praise and thanks are due to Allah S.W.T and peace and blessings be upon his Messenger Muhammad (peace be upon him). First of all, I would like to thank my advisor Assoc. Teacher Prof. Dr OĞUZ BAYAT, for his support, patience, interest, diligence and guidance. his Extensive knowledge helped me to accomplish this task. Also, I am grateful and thankful to my parents and siblings (Abdullah, Yousif, Hussein and Murtadha) who have always encouraged, motivated and supported me in my life. Finally, Thanks for the hospitality we experienced in Turkey and thanks to Altinbas University for providing the skills that enabled us to complete this dissertation. I would like to thank all staff of the Faculty of Electrical and Computer Engineering, for there kindness and cooperation during my studies.

ABSTRACT

BLACK WIDOW OPTIMIZATION ALGORITHM COUPLED WITH AES CRYPTO FOR MULTILEVEL IMAGE THRESHOLDING WITH IMPROVED OTSU THRESHOLDING

AL-RAHLAWEE, Anfal

PhD., Electrical and Computer Engineering, Altınbaş University,

Supervisor: Prof. Dr. Oğuz BAYAT

Date: July / 2023

Pages: 96

Thresholding images, a technique that uses histogram analysis, is an important aspect of the study of image processing. These methods an image's histogram and recommend optimal threshold settings for discriminating between image regions. Since thresholding achieves high accuracy and efficiency, it is widely employed in studies involving picture segmentation. Among the most significant thresholding techniques in image processing is called multi-level thresholding, and it incorporates the Otsu approach, which is utilized by a large number of people. While these approaches are effective and efficient, they are also very computationally intensive. Increases in the number of criteria employed cause these strategies to become less effective because of their increasing complexity and execution time. The Black Widow Spider Optimization Algorithm is one example of a metaheuristic algorithm that can be utilized as part of the Otsu threshold technique to help find good threshold values. These algorithms can determine, in a reasonable time, which thresholds are most effective for a given image. The suggested technique considers each threshold as a constituent or facet of a solution to the Black Widow Spider Optimization Algorithm in order to determine the optimal threshold value with minimal intricacy.

Cryptographic techniques are gaining prominence as a means of guaranteeing safe data transit across a wide range of use cases. As more and more industries begin to rely on visual processes, protecting sensitive proprietary image data becomes more vital than ever. When

it comes to protecting sensitive information, nothing beats the AES, a block cipher that has numerous benefits. In many image processing applications, multilevel thresholding image segmentation is popular. Thresholding uses gray levels to separate an object from its background in photo segmentation. Metaheuristic methods like the Black Widow Optimization (BWO) Algorithm can determine the Otsu threshold. The study's goal is to prove that employing an iris template may provide a cryptographic key that is both secure and difficult to compromise. An iris template or code is generated from the processed iris pictures and utilized for security purposes. During this phase, BWO method is used for image thresholding. For data protection purposes, we segment the iris from an eye image before encrypting and decrypting it using the advanced encryption standard (AES). Experimental results reveal that iris image encryption and decryption techniques were quick and secure. The results reveal that the suggested technique has a higher PSNR index value than the competing algorithms in 83.33 percent of the experiments, and a higher SSIM index value in 80 percent of the experiments. The suggested algorithm's thresholding performance on medical photos like brain tumours and human retinal images is demonstrated by an analysis of a set of pertussis images.

Keywords: Swarm Intelligence Algorithms, Black Widow Optimization Algorithm, Cryptography, Advanced Encryption Standard, Thresholding, Otsu.

TABLE OF CONTENTS

Pages

ABSTRACT……vi

LIST OF TABLES..... X

LIST OF FIGURES…….....xi

ABBREVIATIONS……...xiii

1. INTRODUCTION……1

1.1 OVERVIEW 1

1.2 IMAGE SEGMENTATION 3

1.3 APPLICATION OF IMAGE SEGMENTATION..... 5

1.4 CRYPTOGRAPHY CONCEPT 6

1.5 MOTIVATION 7

1.6 OBJECTIVES OF THESIS 7

1.7 CONTRIBUTION OF THESIS..... 8

1.8 OUTLINES OF THESIS 9

2. BACKGROUND AND LITERATURE SURVEY……...10

2.1 BACKGROUND 10

2.2 LITERATURE SURVEY..... 10

3. THEORETICAL BACKGROUND……...20

3.1 INTRODUCTION 20

3.2 INTRODUCTION TO IMAGE PROCESSING 20

4. METHDOLOGY……40

4.1 INTRODUCTION 40

4.2 PROPOSED SYSTEM 40

4.2.1 Encryption Phase..... 47

4.2.1.1 Segment iris image using otsu thresholding……..47

4.2.1.2 Optimize segmentation using BWO algorithm,,, 47

5. RESULTS…………………………………………………………………………… 50

5.1 OVERVIEW 50

6. DISCUSSION AND CONCLUSIONS…………………………………………….. 74

REFERENCES……………………………………………………………………...76

LIST OF TABLES

Pages

Table 3.1: Distinctions in Segmentation Methods …… 25

Table 3.2: Advantages and Disadvantages of BWO ……..……..…..37

Table 5.1: Implementation Parameters of the Proposed Method and other Algorithms ……61

Table 5.2: The Value of the Objective Function …….……69

Table:5.3 PSNR Value with a Number of Thresholds 1, 2, 3, 4 and 5…….……70

Table 5.4 SSIM Value with a Number of Thresholds ……71

Table 5.5: Standard Deviation Index in Standard Images …….....75

Tablo 5.6: Various Performance Metrics……...…….…...……...81

Table 5.7: Encryption Quality Measurements……...……84

LIST OF FIGURES

Pages

Figure 1.1: Image Segmentation Process. 4

Figure 1.2: Image Segmentation Techniques ….. ……..……4

Figure 1.3: Cryptographic Encryption Algorithms……..……..……8

Figure 3.1: Steps of Digital Image Processing. .. ..…….……..22

Figure 3.2: Flowchart of the Black Widow Optimization Algorithm…..…..……..…33

Figure 3.3: Mutation.... ……..……..35

Figure 3.4: Applications of BWO Algorithm . …..…….……...…33

Figure 3.5: The Classification of Encryption Algorithms…….……39

Figure 3.6: Advanced Encryption Standard Process…..…..……..……40

Figure 4.1: Optimal Threshold by Otsu Threshold…. …..…….……...…46

Figure 4.2: Otsu Thresholding……..…….……..…….47

Figure 4.3: AES Encryption Process of the Proposed System . …..…….…….58

Figure 4.4: AES Decryption Process of the Proposed Syste……...…….……..……58

Figure 5.1: Standard Image Set for Evaluating the Proposed Algorithm....…..…….……60

Figure 5.2: Magnetic Resonance Imaging Set for Evaluating the Proposed Algorithm……60

Figure 5.3: Optic disc Images for Evaluating the Proposed Algorithm…….60

Figure 5.4: Examples of Dataset Images …….…….……61

Figure 5.5: Otsu Implementation on Lena Image.. …….…….……62

Figure 5.6: Implement the Proposed Method on the Lena image with Threshold Numbers 1, 2, 3 and 4. …..…….……67

Figure 5.7: The value of the Objective Function in the Cameraman Image in the Proposed Method . …..…….……...68

Figure 5.8: Comparison of the Average Execution Time in the Proposed Method with other Algorithms..…..……..……..73

Figure 5.9: Comparison of Execution Speedup in the Proposed Method with Other Algorithm…….……...…….74

Figure 5.10: Application of the Proposed Algorithm in the Segmentation Brain Tumors….....77

Figure 5.11: Application of the Proposed Algorithm in Segmentation the Optic Image. …..…….……...80

Figure 5.12: Algorithms Performance Evaluation …...…….……82

Figure 5.13: Threshold Performance Evaluation ..…..…….……...…..…85

Figure 5.14: SSIM Performance Evaluation ..…..…….85

ABBREVIATIONS

BWO	:	Black Widow Optimization Algorithm
BA	:	Bat Algorithm
SSA	:	Salp Swarm Algorithm
PSNR	:	Peak Signal-To-Noise Ratio
RDR	:	Rim-To-Disc Ratio
DDLS	:	Disc-Damage-Likelihood Scale
CDR	:	Cup-To-Disc Ratio
OD	:	Optic Disc
PSO	:	Particle Swarm Optimization
MSSCL	:	Multi-Scale Sparse Coding-Based Learning
RKP	:	Round Key Permutation
MT	:	Multilevel Threshold
HSA	:	Harmony Search Algorithm
SI	:	Swarm Intelligence
BT	:	Bi-Level Thresholding
ASI	:	Artificial Swarm Intelligence
EA	:	Evolutionary Algorithm
GA	:	Genetic Algorithm
CR	:	Cannibalism Rating

PP	:	Procreating Rate
PM	:	Mutation Rate
AES	:	Advanced Encryption Standard
MSE	:	Mean Square Error
SSIM	:	Structured Similarity Index Method
SD	:	Standard Deviation
FA	:	Firefly Algorithm
SOS	:	Symbiotic Organisms Search
ABC	:	Artificial Bee Colony
GWO	:	Gray Wolf Optimization

1. INTRODUCTION

1.1 OVERVIEW

Visual perception is essentially a data-analysis activity. The data must be converted into a format understood by the visual processor before it can be used. It is the rods and cones in the human retina that perform this function. The cornea is the transparent window through which external light enters the eye, where it is then focussed by the lens and reaches the retina. Here, light energy is transformed into a signal via an electrochemical process in the rods and cones [1]. The brain receives this signal after it has travelled along the optic nerve. The brain processes the signal by converting it into electrical activity patterns that are subsequently interpreted as a picture. It is also possible to use a computer to complete a task that is similar to one that would be performed by hand [2]. In order to turn light into an electrical signal, a photosensitive gadget lets light flow through it. This digital representation of the electrical signal can then be sent to a computer and used to generate an image. Even though the computer can snap a photo, it has no idea what it captured. To aid in such circumstances, computer vision can be used. The term "computer vision" is commonly used to describe the academic discipline that seeks to automate and integrate a wide range of the processes and representations that are used for visual perception [3].

Captured images have helped solve many problems in earth science, physics, biology, business, and other fields that were previously unsolvable using traditional methods. Images have also played a role in the growth of medicine, the most crucial field for ensuring the survival of the human race. There is a rising need for automated image analysis, processing, and recognition due to the growing significance of images [4][2]. The need for processing arises from the possibility that the images cannot be re-captured, either because the phenomenon cannot be reversed or because it is too expensive to repeatedly capture the same image. Because of this fragmentation, the development of digital image processing was inevitable [5].

When taking in visual information, the process of scene segmentation is essential. Successfully, this method reduces complex scenes to a list of objects that can be handled individually [6]. The process is described by digital image processing, which involves segmenting the image into many discrete regions, each of which represents a set of pixels and each of which represents an entity, and then applying various filters to each of these

subsets. Image segmentation technology is used to complete the procedure, it is an important intermediate step between image processing and image analysis [7].

The literature suggests a number of techniques for data and image extraction. In the segmentation approach, thresholding has attracted the most attention among the aforementioned methods. The threshold method is a simple and effective technique for isolating relevant data from surrounding noise. It is used in document image analysis to extract text [8], logos, graphics, or musical scores, and in map processing to pinpoint line endings, legends, and characters. It has also been applied to scene processing for the purpose of object labelling and recognition, and to quality inspection for the elimination of defective components in materials [9]. Based on their segment region count, threshold techniques are bi-level or multi-level. Bi-level thresholding categorizes pixels into object and context [10]. Numerous bi-level thresholding methods have been established by scholars using various approaches such as histogram, edge detection, variance, interactive pixel categorization and two-dimensional techniques [11]. Entropy-based global thresholding methods work very well for the great majority of real-world photos. The histogram of an image, which includes both the foreground and background, is used as the basis for entropy-based global thresholding [12]. When used with bi-level thresholding, the stated entropies yielded helpful segmentation results. Since it uses a global threshold, bi-level thresholding can fail in situations when there are several artifacts with different contrast levels [13]. The use of multi-level thresholding strategies received more focus from the research community. It is possible to divide an image into distinct areas using a method called multilevel thresholding. In this technique, various thresholds are used to segment an image into a shared background and individual object sections. Even with complicated settings, multi-level thresholding provides reliable results [14], where bi-level thresholding often fails to produce desirable results. Researchers were motivated to investigate different levels for complicated coloured images after seeing the success of multi-level techniques for grayscale images [15]. Due to their useful properties, such as low memory and processing requirements, thresholding methods are increasingly being considered for efficient image segmentation in a wide range of contexts. Various techniques, such as Swarm Intelligent Algorithms, can be used to determine the best pixel thresholds [16], making image segmentation with multilevel thresholding a mature subfield of image processing. The increasing prevalence of high-complexity problems that demand sub-optimal but still doable in a reasonable amount of

time has contributed to the rise in popularity of swarm intelligence, a core component of artificial intelligence. An example of AI, swarm intelligence models the behaviour of a herd of animals in a survival situation. Biological processes have a disproportionately large impact on it [7][17].

1.2 IMAGE SEGMENTATION

Computer vision relies on the segmentation technique to divide a digital image into clusters of similar pixels. The purpose of segmentation methods is to produce an image that is both simple and meaningful. The human visual system has impressively precise segmentation abilities. The advantages of automated segmentation methods outweigh their drawbacks, which include lower accuracy and less generalizability than human-performed methods. In order to find appropriate partitions of an image, automated methods perform complex mathematical analysis[18][19].

With automation, the procedure can be run over a large number of photos repeatedly in the hopes of achieving uniform outcomes each time. Due to advancements in computing power, segmentation algorithms can now be executed in a practical amount of time. Over the past few years, segmentation techniques have seen a surge in their widespread adoption. These segmentation techniques have spread into many different fields and found a wide variety of applications because many generic approaches make no assumptions about the nature of the information contained in the original image[20]. Segmentation methods in medical imaging aid in tumour detection, diagnosis, and treatment planning. Segmentation methods are also used in fingerprint scanning and facial recognition techniques [21][22]. Although low-level information such as texture and colour are considered by some segmentation algorithms, pixel intensity is often employed as the primary source of contrast. Graph-based methods have become increasingly common for performing segmentation [23]. When performing image analysis, it is useful to conceptualize the image as a weighted undirected graph, where pixels serve as nodes and the intensities of the edges between neighbouring pixels serve as edge weights. There are numerous metrics that may be used to an image in order to determine what details are crucial. Some scenarios may not be suitable for the time-consuming and idealistic graph-based solutions outlined in [24][25].

The segmented image shown in Figure (1.1) was made by cutting the original image into sections that shared the same level of detail in their pixels. An effective approach is utilizing

a segmentation methodology in instances where the outputs' pixels exhibit unique characteristics, such as discontinuity and similarity properties. Additionally, it would be appropriate to employ this technique when said pixels correspond to multivariate values or form regions associated with specific shapes [26]. Edge detection, thresholding, neural networks, and k-means clustering are common segmentation approaches. Figure (1.2) shows picture segmentation techniques.

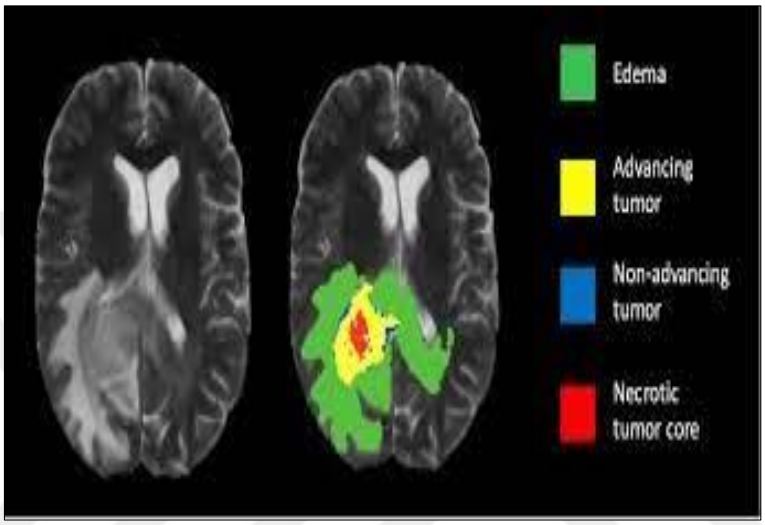

Figure 1.1: Image Segmentation Process [8].

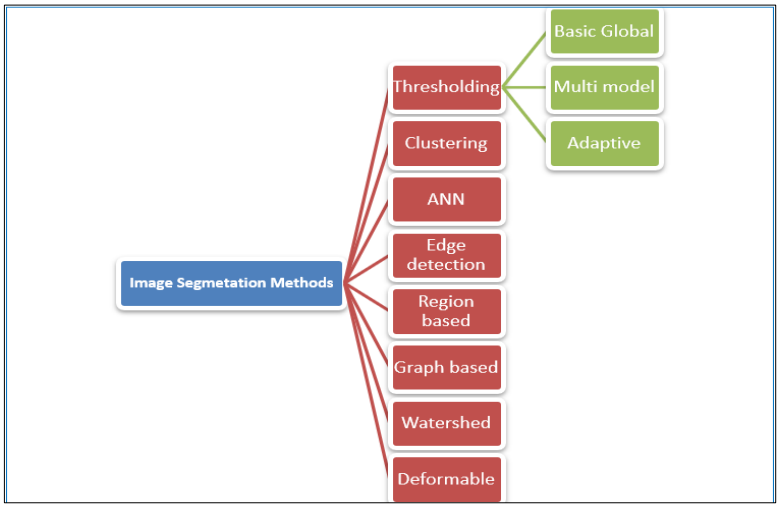

Figure 1.2: Image Segmentation Techniques [10].

When it comes to segmentation, using a multilevel approach can help to speed things up. Multilevel approaches use coarse approximations of the underlying problem to reduce calculation time. A multilevel technique's computational overhead usually grows linearly

with the number of pixels, which is the number of variables in this case. Since photos include numerous pixels, this is helpful. This thesis presents a new method for detecting salient regions in images using Otsu multilevel graphs, which incorporates low-level visual cues such as intensity, colour, and texture, as well as higher-level cues such as shape. This new metric appropriately accounts for scaling across dimensions. In order to address segmentation issues in medical imaging, this thesis seeks to implement a hybrid Otsu - Black Widow Optimization Algorithm (BWO) algorithm.

1.3 APPLICATION OF IMAGE SEGMENTATION

The process of segmenting an image involves breaking it down into smaller, more manageable pieces. Segmentation is a technique used to divide large images into smaller, more manageable pieces for improved analysis. Partitioning an image into regions that are substantially linked with regions of interest is the fundamental goal of segmentation. Despite the fact that thousands of algorithms exist, none of them are universally useful because they don't address every possible digital image type or accomplish every possible goal.

1.3.1 Medical Image Segmentation

The process of segmenting medical images has many practical uses. In the field of medicine, it is used for tumour analysis and localization, anatomy analysis, and other similar tasks. It has an equivalent or higher resolution in both brightness and contrast. In the realm of image processing and analysis, partitioning is a significant obstacle that necessitates resolution [27].

1.3.2 Thresholding

Threshold segmentation, a common method of parallel segmentation, is both the simplest and fastest way to divide an image into separate parts. The local and global threshold segmentation methods are independent [28]. Thresholding is a vital technique for dividing images into distinct parts. In light of the fact that thresholding produces a segmented image. As opposed to a grayscale image with 256 levels, which requires more storage space, processing time, and effort to manipulate, thresholding techniques have become increasingly popular in recent years due to their advantages [29]. Segmentation's goal is to eliminate

distracting backgrounds and increase contrast by identifying and separating foreground objects from those in the background. The idea that neighbouring pixels in an image indicate the same item and so share comparable qualities (like brightness, contrasting, and colour) is central to many images processing tasks. This hypothesis suggests that segmentation may be possible [30].

1.4 CRYPTOGRAPHY CONCEPT

Cryptography employs mathematical and engineering principles to secure communication via insecure channels. It uses encryption and decryption operations to transform plaintext into ciphertext, which unauthorized parties cannot access. This fundamental tool underlies modern security systems [31]. Therefore, it will be difficult to restore files to their former condition unless the key used in the encryption method is known [32]. The fundamental components of a cryptosystem comprise the cryptographic technique, also referred to as an algorithm, alongside its corresponding key. In terms of quantity, a method is composed of several actions and possesses a secrecy characteristic that modifies data. The primary impetus behind the creation of cryptography stemmed from the need to ensure secure functions including but not limited to non-repudiation, confidentiality, authentication,

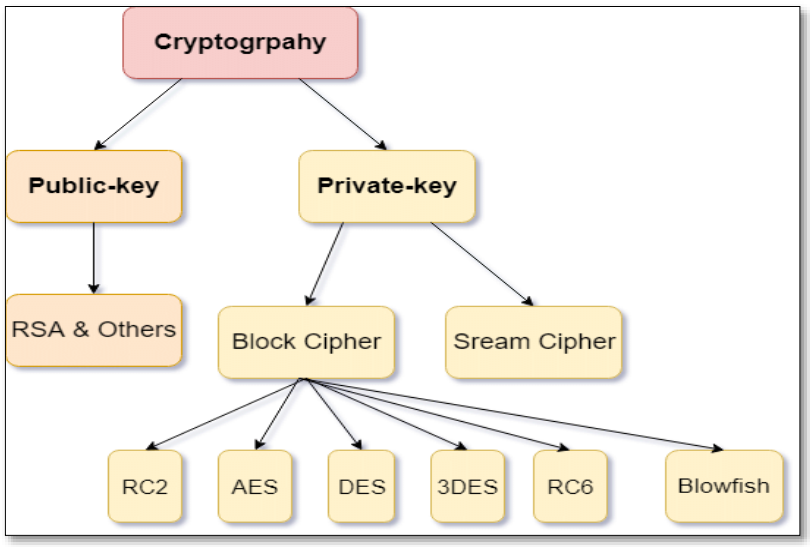

Figure 1.3: Cryptographic Encryption Algorithms [34].

authorization and preservation of data integrity [33]. The image depicted in Figure (1.3) highlights the differentiation between asymmetric, also known as public key encryption

algorithms and symmetric or secret encryption algorithms which are the fundamental types of cryptographic algorithms employed for securing data.

1.5 MOTIVATION

This research aims to create a hybrid segmentation algorithm that can efficiently segment images with minimal human interaction. The process of segmentation that is used in computer vision is extremely adaptable, and specific segmentation techniques have been created to accommodate a wide range of different use cases. The driving force behind this study was the need to develop a segmentation technique that can be applied to various contexts with minimal tweaking of the underlying parameters. With its flexible framework, the Otsu algorithm is easy to adapt to specific needs. The algorithm's flexibility stems from the fact that many different types of visual signals can be used in the segmentation process. To some extent, the multilevel approach can be compared to the way humans see. Bottom-up segmentation techniques, which rely solely on simple visual characteristics of an image like colour and texture, are the most common. As a multilevel approach, the Otsu method allows for the incorporation of high-level vision cues into the segmentation procedure. Top-down approaches utilize prior information about the subject matter of a picture to guide the segmentation procedure. The segmentation process can then take into account high-level visual cues like shape and orientation. Otsu is an algorithm for image segmentation that combines some features of both bottom-up and top-down approaches.

1.6 OBJECTIVES OF THESIS

Segmenting an image means dividing it up into smaller sections that represent individual objects, surfaces, or anatomical features. Image segmentation is seen as an ill-posed problem by the majority of the computer vision community. When there is no uniformity in how objects are understood, determining the correct segmentation can be difficult. Low-level features and a bottom-up strategy characterize conventional methods of image segmentation. They frequently over-segment due to a deficiency of global and high-level data providing object-related awareness. Finally, the information provided about object definitions is tightly intertwined with the segmentation tasks. Numerous well-defined and context-specific image segmentation tasks are currently available for use in a wide range of settings. Depending on the ultimate purpose, a different representation of the image function may be necessary.

Feature representation methods, however, are relatively close. However, there is currently no comprehensive work that addresses the broad range of segmentation tasks. Therefore, this thesis's goals are:

a. The foremost purpose of this thesis is to propose a general concept for solving the issue of multi-level image segmentation and thereby attempt to close the gap in the literature on this topic.
b. Explore the application of swarm intelligence techniques (the Black Widow Algorithm) to the problem of multi-level image segmentation and the outcomes that this approach yields.
c. Use swarm intelligent approaches to recycle pre-existing sources and decrease data needs without compromising performance.
d. The use of AES Cryptography in conjunction with Otsu thresholding techniques to strengthen image security.

1.7 CONTRIBUTION OF THESIS

This thesis includes the following primary contributions:

a. Specifically, this thesis demonstrates how to combine multi-level thresholding with elements of swarm intelligence. When compared to other swarm methods, the proposed approach produces superior segmentation results.
b. With minimal use of complex mathematics, has been made to streamline the terminology around several of the most crucial techniques for image segmentation.
c. This research employs a multi-level thresholding scheme to help the user comprehend the fundamental similarities and differences between thresholding approaches to image segmentation.
d. Using AI algorithms, and more specifically swarm algorithms, for image segmentation allows for greater accuracy and the ability to segment images according to predetermined criteria, leading to improved image quality.
e. Finally, the primary areas of application have been investigated so that AES Cryptography and Otsu thresholding techniques can be used to bolster image security.

1.8 OUTLINES OF THESIS

This thesis is broken up into six different sections. The next few paragraphs contain a synopsis of each of the remaining chapters in the thesis. Chapter Two: A survey of the relevant literature covers the work done by earlier researchers in a variety of different time periods. Chapter Three: The theoretical background explains key concepts and offers an overarching perspective on image processing, image segmentation, swarm intelligence algorithms, and their primary application areas. It also defines key terms. Chapter Four: The suggested design of the system is thoroughly elaborated by delineating its configuration and organization in great depth. Chapter Five: The execution and outcomes of the suggested system are analysed in relation to different approaches recommended for evaluating its efficiency. This evaluation also highlights the distinctions between such methodologies. Chapter Six: This chapter presents the research conclusions and the derived suggestions for further study.

2. BACKGROUND AND LITERATURE SURVEY

2.1 BACKGROUND

Image segmentation, a technique used to extract valuable information by dividing an image into several parts, is a crucial method that faces various challenges. these difficulties arise due to the impact of factors such as artifacts (like partial volume effect and noise) and image degradation (such as blurring or color imperfection). this process presents significant complexities despite its usefulness in critical areas like medical imaging, traffic control systems, video surveillance platforms among others. while people have been aware of the intricate nature of this task for some time now, it remains one of the most formidable undertakings concerning object detection and photo analysis producing great implications on final results' accuracy.

2.2 LITERATURE SURVEY

The topic of image segmentation has been extensively studied by many researchers who have conducted numerous experiments in search of viable solutions. A plethora of approaches to this problem rely on various types of software for image segmentation. One widely used clustering algorithm is K-means, which is considered the most straightforward approach; it remains popular and relevant today, with a diverse range of methods employed to set up the cluster centre. A large number of scientists are actively participating in the effort to develop methods that can advance existing practices and techniques. The central hypothesis of the thesis as well as the methodology will be supported by the following summary of the research. The following research is presented in reverse chronological order, beginning with the most recent publication and working backwards. Verma and Malhotra (2017)[35], offered another AES encryption/unscrambling security demonstration. It depends on either the selective encryption method AES Key Expansion or the functioning of an image pixel layout that uses a unique 128-piece key. When AES encryption is being used, both the sender and the receiver are in possession of the secret key. Even if an eavesdropper has access to both the plaintext and the ciphertext, the AES algorithm is still secure because the key cannot be retrieved using any method that is currently known. Arab et al., (2018)[36], devised is a fresh image encryption approach that employs an upgraded

variation of the AES algorithm along with chaos sequence. The chaotic progression generates the encryption key in this manner. Subsequently, modified version of AES and round keys derived from chaotic system encrypts input images instead. This novel technique eradicates temporal intricacy while introducing diffusion to secure encrypted images against differential attacks effectively. Furthermore, it has been proposed that implementation of such methodology provides much larger space for keys which make them resilient towards brute-force assaults as well. Abdullah et al., (2018)[37], suggested that a new pre-processing retinal picture employing an improved bat algorithm (BA) may be utilized to find the optic disc in the image of the retina. Grayscale conversion is performed on the image in its entirety during the pre-processing step so that it can be viewed in only its grayscale form. After this step, morphological operations are applied to the images in order to eliminate shadowy components such as blood vessels. After that, the bat algorithm, also known as BA, is applied in order to identify the ideal threshold value for the optic disc spot. In the last phase of the process, the elliptical fitting approach was utilized to tighten and smooth the boundary area of the segmented optic disc. This was done in order to ensure that the boundary area would not be damaged. During this stage, the objectives were to improve the precision of the segmented optic disc and achieve the best potential result that could be achieved. The technique of decreasing the squared distance between the points is applied in order to carry out the process of fitting an ellipse to the data. MESSIDOR, DRIVE, DIARETDB1, DIARETDB0, STARE, and DRIONS-DB are all datasets that are available to the general public, and the suggested method was tested on these datasets. In these six databases, the average overlaps and precision for optic disc segmentation were 78.5–88.2% and 96.6–99.91%, respectively. The retinal images ‘optic disks were segmented in less than 2.1 seconds per image.

Narasimhan and Arunachalam, 2019[38], discussed the utilization of unclonable PUF-based true random numbers to strengthen unique authentication methods in iris verification. Non-reversible MAC codes are created by using both Discrete Wavelet Transform and PUF features specific to iris biometrics. In addition, encryption algorithms provide additional confidentiality for individual iris identification. Experiments conducted with CUHK Iris Image Dataset show that this proposed Bio-PUF system provides significant functional advantages regarding the production of an unclonable pseudo-random number through its use of PUFs. To evaluate performance against a range of parameters including avalanche

effect, entropy, NCPR and UACI metrics, analysis was performed on crypt functions based on PUF data from experimental results. It is reported that with enrolment using Bio-PUF-MAC codes for 75% matching accuracy during correct identification reaches up to 77.73%. Pathan et al., (2019)[39], developed an innovative method for accurate segmentation of the optic disc by detecting blood vessels and disregarding them in the process. There are two different approaches one might take to finish this task. Using a directional filter, an efficient method is first constructed in order to discover blood vessels and then eliminate them from the analysis. In the second stage, a decision tree classifier sets an adaptive threshold for optic disc contour detection. The method also segments the optic disc in fundus photos with illuminations, reflections, and exudates computationally. The KMC dataset has an average Jaccard index of 91.28 percent, dice coefficient of 94.17 percent, sensitivity of 92.71 percent, specificity of 99.89 percent, and accuracy of 99.61 percent. The RIM-ONE dataset averages 85.30 percent Jaccard index, 90.69 percent dice coefficient, 93.90 percent sensitivity, 99.50 percent precision, and 99.15 percent accuracy.

Zhou et al., (2019)[40], suggested a more effective line detector, which was implemented to efficiently extract the primary vessel structures. Next, we use the HMM to detect vessel centrelines, including those of thin vessels. Finally, the approach is de-noised, and the two vessel styles are combined, resulting in complete segmentation results. Two public databases (DRIVE and STARE databases) and five metrics (accuracy, sensitivity, specificity, the Dice coefficient, the structural similarity index, and the feature similarity index) are used to assess the performance of the proposed segmentation method (FSIM). The DRIVE dataset has values of 0.9475, 0.7262, 0.9803, 0.7781, 0.9992, and 0.9793 for the aforementioned performance metrics, while the STARE dataset has values of 0.9535, 0.7865, 0.9730, 0.7764, 0.9987, and 0.9742.

Derwin et al., (2019)[41], Presented is an inventive approach for detecting both micro and non-micro-aneurysms through a process that involves image pre-processing, candidate extraction, feature extraction, and classification. To capture the texture-based attributes of micro-aneurysms in this method, a generalized rotationally invariant local binary pattern serves as the feature extractor. Results indicate that when compared with shape-and color-dependent features, GRILBP derived features offer higher accuracy in MA detection along with improved output per lesion and per image analysis capability. Additionally, this technique is demonstrated to distinguish between MAs from non-MAs with superior

performance outcomes on ROC datasets; FROC scores are 0.421 versus LBP's earning of only 0.410 score points obtained by employing regular methods like LBP.

Wang et al., (2019**)**[42], proposed a modification for the slap swarm algorithm to improve its effectiveness in multi-threshold picture segmentation. While employing a multi-threshold approach can result in impressive outcomes, precision may diminish as thresholds increase. To address this issue and attain more precise segmentation rates, the SSA is employed initially to determine optimal fitting function parameters, followed by an additional enhancement through levy flight mechanisms. Fitness functions such as Kapur's entropy, Otsu's entropy and the Renyi entropy are utilized during optimization stages to rank solutions appropriately. The investigation also involved analysing information using peak signal-to-noise ratio, feature similarity index measurements, and best fitness values attained during experimentation procedures.

Kumar et al., (2019)[43], created a different and totally automated fundus image processing method using the rim-to-disc ratio for glaucoma screening (RDR). Before computing the RDR, the method precisely segments the optic disc and optic cup, allowing it to distinguish between normal and glaucomatous fundus's. During the operation, the patient's score on a disc damage scale determines the severity of their glaucoma (DDLS). The active disk segments the optic disc and cup for maximum regional contrast. Using sensitivity, specificity, accuracy, Jaccard, and Dice similarity indices, segmentation and classification performance is compared to expert clinician annotations. RDR-based automatic glaucoma assessment is 8-10% more accurate than cup-to-disc ratio (CDR). Four test datasets had 100% accuracy.

Jianbo et al., (2019)[44], introduced a new strategy for developing an AI-powered system for the detection, classification, and quantification of disease. The technique does more than just diagnose the condition; it also analyses the disease's usual pathological aspects in depth, which helps clinicians make better decisions and communicate those decisions more clearly. Retinal blood vessels were isolated from the optic disc with the aid of a deep learning network (OD). Vessel segmentation-based assessments of tortuosity, breadth, fractal dimension, and vessel density were also performed automatically, and disease classification was accomplished. The qualified network's sensitivity was 95.1 percent and its precision was 97.8 percent when diagnosing plus disease. The detection rates of periplus or worse were 92.4% sensitive and 97.4% specific. The quadratic weighted k was 0.9244.

Kiran et al., (2020)[45], presented a methodology for selective image encryption called the Region of Interest technique. The method involves an active contour segmentation process to separate the ROI from the Region of Background. A Permutation-diffusion scheme using Hilbert curve and Skew Tent map is employed on pixels within the ROI region, with permutation based on a Hilbert scanning pattern, followed by XOR operation between random numbers generated through predetermined threshold values originating from skew tent maps. The encrypted blocks are formed at last through combining respective ROIs and ROBs. Results obtained illustrate that this proposed approach exhibits enhanced data security attempting to mitigate risks relating correlation checking, key sensitivity analysis as well as formulating entropy, diffusion characteristic measurement and histogram evaluation methodologies in cryptographic research domains.

Shalaby et al., (2020)[46], introduced a new method for encrypting medical images using chaos theory. To preserve the intricate details of the image during encryption and decryption, a Butterworth High Pass Filter is applied first. The proposed approach enhances Arnold's cat map technique by including an Advanced Encryption Standard algorithm while adding three bits to improve overall encryption security. This modification increases robustness against potential attacks on encrypted data with greater effectiveness than previous methods relying only on AES algorithms or standard chaotic mapping techniques such as Arnold's cat map alone.

Devarajan et al., (2020)[47], proposed a technique to detect ocular disorders that could indicate the future occurrence of serious ailments such as hypertension, cataracts, diabetic retinopathy and age-related macular degeneration. The method involves using a three-phase neural classifier that adopts machine learning principles for identifying whether a specified pixel in the search area pertains to a blood vessel or not. Further, ant colony optimization is applied to determine the optimal feature vector assortment before implementing classification models with high-end targets for improved efficacy of pattern recognition by neural networks. The originality and value of this approach lie in its back-tracing segmentation scheme, which enhances the pre-processed features prior to categorizing them for segmented analysis. This eliminates redundant feature vectors that might consume considerable memory and raise computational overheads. The technique is assessed on 30 instances, comprising equal numbers from two popular databases, via automated learning

algorithms. On average, accuracy rates exceed 96% for segmentation classification and reach almost 99% for anomaly detection tasks.

Abdel-Hamid (2020)[48], used wavelets to create a glaucoma screening algorithm that could work in real-time. Wavelet-based statistical and textural factors from the optic disc area define a retinal image's stability or glaucomatous ness. We used two open-source datasets of varying detail to test the suggested method. The high-resolution data set had 96.7 percent accuracy and 94% AUC. Using three distinct types of analysis, it was determined that wavelet-based statistical and textural variables were significant for glaucoma identification. Processing high-resolution retinal images with the proposed algorithm takes less than 3 seconds, proving its suitability for use in real-time settings.

Ramani and Shanthamalar, (2020)[49]**,** developed a refined algorithm for processing retinal fundus images cantered on identifying and segmenting optic discs using a region-based pixel density estimation technique, an upgraded Circular Hough Transform with Hough Peak value selection, and Red Channel Super pixel segmentation. The accuracy rates of the proposed approach were evaluated using eight publicly accessible datasets including HRF, DRISHTI-GS1, DRIONSDB, DRIVE, ONHSD CHASE-DB1., INSPIRE and MESSIDOR obtaining impressive results with respective percentage scores of 99.73%, 99.31%. 99.37%, 99.38%, 99.64%, and specificity values ranging from (insert specific percentages) cent respectively.

Dharmawana et al., (2020)[50], introduced an automated method for detecting the optic disc boundary in fundus images through segmentation. Optic disc candidates were identified using a modified Dolphy-Chebyshev filter that matched features. The circular Hough transform and B-spline approximation techniques were applied to accurately outline the optic disc's boundaries. This method can be implemented on various regions of interest such as template-based, vessel-density map-based, and maximum-entropy based locally-defined areas by utilizing matching filter, Circular Hough Transform, and B-spline approximation approaches. Testing was carried out on MESSIDOR and DRIVE datasets with superior results achieved above 99 percent accuracy in identifying optic discs using this proposed technique.

Durai and Raja, (2020)[51], proposed a novel Particle Swarm Optimization (PSO) optimized KNN used for glaucoma disease classification. PSO is a naturally inspired optimization algorithm that can be used to find KNN optimization parameters and increase classification

accuracy. The proposed algorithm consists of three distinct stages. Histogram equalization is used to improve contrast and reduce noise during the pre-processing stage. The OD detection method used was FCM. The Optic Disc images were then classified as healthy or unhealthy using the PSO-KNN classifier. The proposed method was evaluated using the DRIVE and STARE fundus image datasets. The results demonstrate a dramatic improvement in accuracy using the proposed approach, with a 98.3 percent success rate.

Khan et al., (2020)[52], presented a novel, fast, and robust method for OD localization and segmentation. The proposed solution involves de-hazing the image before cropping out the OD region. After the image is cropped, it is transformed to the HSV domain so that the V channel can be examined for OD symptoms. In order to remove the blood vessels from the green channel in the cropped area, a multi-scale line detector is employed to extract them, and then the Laplace Transform is applied. It is proposed to first filter off unwanted background details from the image, and then use the eccentricity and field attributes of areas to pinpoint the actual OD spot. After that, an ellipse that is the best fit for the data is used to fill in the region. The efficiency of the suggested strategy is tested on a variety of datasets. The obtained precision for these datasets is 99.5% for DIARETDB1, 99.2% for MESSIDOR, 99.5% for DRIONS-DB, 99.5% for Drishti-DB, 99.5% for RIM-ONE-DB, and 98.9% for ONHSD.

Hayyolalam and Kazem (2020)[53], presented a Black Widow Optimization Algorithm (BWO) based on black widow spider mating behaviour. This method requires cannibalism. Early convergence occurs when unfit species are excluded from the circle. The BWO method is assessed against fifty-one benchmark functions to determine how well it finds the best solutions to various problems. The results show that the algorithm achieves early convergence and optimum fitness values. It also has competitive and promising results. The results show that the algorithm solves real-world problems in unfamiliar and complex regions.

Shahabi et al., (2020)[54], integrated Otsu and CSA to speed up multi-level thresholding and improve segmentation. Only combining the two methods made this possible. Otsu helps the CSA algorithm segment data by increasing class variance and decreasing class variance. The proposed model has the lowest computational time. Other models include the FA composition model, fuzzy FA model, and PSO model with the Otsu process. In conclusion,

the newly designed hybrid algorithm segmented gray-level images accurately and in real time due to its optimal computing time.

Zhe et al., (2020)[55], solved the Optic Disc problem with coarse-to-fine segmentation. After building a U-Net to acquire a crude segmenting boundary, it crops the space along the border to create a contour-centred boundary representation. Second, we employ SU-Net, a unique fully convolutional network, to treat OD and OC segmentation as a sequence labelling problem. This network and Viterbi decode the segmentation border. NLP sequence labelling influenced this method. It also proposes a geometric parameter-based data augmentation technique to increase training samples and reduce overfitting and discrepancy. The Drishti-GS dataset for glaucoma screening had a best cup-to-disc ratio (CDR) error of 0.047 and an AUC of 0.935. These glaucoma classifications are good.

Simrandeep et al., (2020)[56], introduced Otsu and Kapor's entropy MT goal functions into the LebTLBO algorithm for image segmentation. The multilevel thresholding strategy with MLTLBO and Otsu and Kapur's entropy methods were employed as goal functions during histogram-based picture segmentation to preserve more image information. Done. LebTLBO performs well in PSNR, mean, threshold values, number of iterations to converge, and picture segmentation efficiency, according to qualitative experimental data.

Chen et al., (2020)[57], advised retraining the IRB with an MSSCL algorithm. To detect a wide range of abnormalities in a retinal examination image, you must learn the image's individual retinal background (IRB), on which retinal lesions appear. MSSCL sparsely encodes the test image on several scales utilizing language learned from normal retinal images to provide a background space with more IRB information than any single-scale coding result. Low-rank context space approximation can train the IRB to identify and separate significant lesions. The suggested approach surpasses state-of-the-art algorithms by a wide margin (Mean = 0.9918, Standard Deviation = 0.0028).

Bisneto et al., (2020)[58], proposed a new approach for detecting glaucoma in its earliest stages by using a Generative Adversarial Network in tandem with texture attributes determined by taxonomic diversity indices. The steps of this procedure can be broken down into five distinct categories. First, acquiring pictures from public sources like RIM-ONE and Drishti-GS. secondly, segmenting optical discs into retinal images via training a constrained Generative Adversarial Network. Thirdly, fixing flaws and adding polish through enhancement and patching in the pre-processing stage. Forth, the index of taxonomic

diversity is used to extract texture attributes. Finally, the proposal is validated by a thorough analysis of three classifiers using four different measures of effectiveness. Initial accuracy of 79% is encouraging and suggests that the approach is robust. However, after making some tweaks to the methodology, we were able to achieve a ROC curve of 1 and a success rate of 100%.

Romero-Arellano et al., (2021)[59], developed a medical image encryption/decryption algorithm based on three components: Jigsaw transform, Langton's ant and deterministic noise addition. The Jigsaw transform is used for concealing visual information efficiently, while the combination of Langton's ant and deterministic noise results in a reliable and secure approach. A zero mean square error between the original and decrypted images was achieved when tested with high-resolution retinal fundus images as a case study. Several methods were employed to ascertain its efficacy including statistical analysis (histograms and correlation distributions), entropy computation, key space assessment, differential attack robustness test, key sensitivity analysis which individually demonstrate that it offers superior security level. Furthermore, the technique was evaluated against other approaches and exhibited a competitive performance with a keyspace greater than $1 \times 101,134,190.38$. Moreover, it demonstrated robust handling of high-resolution images by achieving entropy values ranging from 7.999988 to 7.999989, an average NPCR of 99.5796% ±0.000674 and a mean UACI of 33.4469% ±0.

Praveena and GaneshBabu,(2021)[60], proposed approaches for computationally determining the cup-to-disc aspect ratio. First, the optic disc area of the fundus image is analysed. When clustering, the optical disc is automatically retrieved using a value (K) selected in an automated method by a hill climbing algorithm. Elliptical and morphological fitting refined the optic cup segmented form. The cup-to-disc ratio is calculated using 50 glaucoma patients' routine and fundus scans. Ophthalmologists provided cup-to-disc ratios for the identical photographs. These values were the reference benchmark for measuring precision. K-means clustering has a mean error of 4.5 percent for elliptical fitting and 4.1 percent for morphological fitting. Elliptical and morphological fitting have fuzzy C-mean clustering of 3.83 and 3.52 percent. In conclusion, the SWFCM clustering approach for morphological fitting has a 1.67 percent mean error and 3.06 percent for elliptical fitting.

Rimani et al., (2021)[61], proposed a new approach in ensuring secret diffusion for image encryption through Round Key Permutation. This strategy applies non-linear, dynamic and

pseudo-random permutation on image blocks as they present various unique characteristics such as large size and information volume, coupled with two dimensions, significant redundancy and intense correlation. The creation of the RKP table involves both primary and secondary keys to generate permutations which are subsequently applied to rearrange encrypted block pixels randomly. Ultimately, AES serves its purpose in providing data security.

Srikanth and Bikshalu, (2021)[62], proposed an energy curve-based multilayer threshold (MT) solution to solve the drawbacks of histogram-based image segmentation. Energy curves derived the way. Histogram-based techniques cannot account for spatial contextual knowledge when Otsu's MT methodology is used with the Harmony Search Algorithm (HSA) to generate optimal threshold levels. HSA cut-off values are calculated by maximizing inter-class variance. The energy curve increased PSNR values and saturated object functions faster than the histogram. The proposed technique has a lower SD index, which implies better scattering of regions or clusters, and a higher MEAN of object function. These two results suggest that the proposed approach merits further refinement.

3. THEORETICAL BACKGROUND

3.1 INTRODUCTION

Given the proliferation of computing power, image processing has found applications in many previously unrelated disciplines. Segmenting images is a well-known challenge in the realm of image processing. Sub-regions of the original image are defined based on intensity, colour, texture, and other visual qualities. Segmentation is a common first step in the processing of images before moving on to more complex tasks like analysis, recognition, or computer vision. Consequently, the efficacy of high-end processing systems is dependent on the precision of the segmentation method employed [63][64]. Researchers have suggested various techniques for image segmentation, such as edge detection, histogram-based thresholding, regional analysis, feature group identification and the utilization of neural networks. The widely-used and primary strategy involves applying a thresholding technique to an image's data-histogram. Multi-level and bi-level threshold methods are typically employed in this approach where only one value is used by binary level threshold type, unlike conventional applications utilizing standard methodology where foreground-background separation occurs through different numbers. Employing multiple thresholds improves the accuracy of image classification significantly [65][66]. Contemporary techniques for image thresholding comprise Otsu and Kapor's entropy algorithms, which involve the optimization of multiple characteristics. Kapor's method maximizes histogram entropy, whereas Otsu realigns with maximum class variance. Leveraging diverse thresholding methods simplifies multilayer segmentation through thresholding. Given that exhaustive searches have an exponential time complexity in proportion to the number of thresholds, they are unfeasible [67][68]. Multilevel thresholding situations often use swarm intelligence (SI) methods to compensate for this limitation. BWO is a swarm approach. Black widow spider mating patterns inspired this algorithm. The Australian Black Widow, or redback spider (Latrodectus Hasselti), evolved in arid South and Western Australia [69].

3.2 INTRODUCTION TO IMAGE PROCESSING

A computer is used to perform the majority of the work involved in digital image data processing, which begins with converting the image signal into a digital signal in one of

several formats. Information gathered by this technology is typically in the form of two-dimensional data, which requires both a large amount of storage space and a fast computer [70]. The field of digital image processing has had far-reaching effects on modern culture. The ability to process digital images is essential in the medical field for the diagnosis of many different conditions. Digital image processing entails a number of steps. Just some of the steps include acquiring the images, processing them, segmenting them, and then classifying them [71] . While each step in the image processing pipeline is important, image segmentation stands out as particularly pivotal. With a properly segmented image, the accuracy of the classification process is enhanced. The steps required for digital image processing are shown in Fig. (3.1).

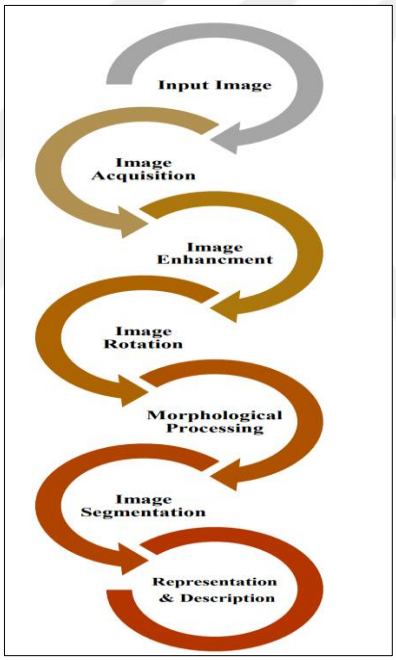

Figure 3.1: Steps of Digital Image Processing[3].

Image segmentation refers to a method whereby an image is cut up into smaller, more manageable pieces for closer inspection of its constituent parts. The characteristics of each component are identical. Parts of images of interest can be isolated for further analysis at a later time. A number of techniques exist for segmenting images.

3.3 IMAGE SEGMENTATION TECHNIQUE

Segmenting images is a common first step in the pre-processing phase of most computer vision systems. It is the image pre-processing quality that sets the bar for how reliable the

final result is. In order to lessen the impact of noise, visual artifacts, and redundant information, studies are focusing on ways to enhance the quality of input images. Segmenting images is a popular approach to these problems. It divides pixels into separate sections. These clusters, each of which stands in for a different thing in a picture, make it possible to learn more about everything there is to learn about what's there[72]. In recent years, image segmentation has found application in many different areas, from medical imaging (such as MRI scans for detecting brain tumours or studying neonatal brain development) to biometric fingerprint enhancement, landscape analysis of remotely sensed satellite images, and object detection in both still and moving images. Both discontinuity-detection and similarity-detection based methods can be used to segment images. Both methods segment an image into regions, but the former uses discontinuity to do so, while the latter uses pixel similarity [73][74]. In order to segment an image, one can use any one of the following techniques[16].

a. Thresholding**:** Thresholding is a method for segmenting images that involves making adjustments to the image's pixels in order to improve readability. Thresholding converts grayscale to binary.

a. Normal Thresholding**:** Segmentation in accordance with the bimodal histogram, as proposed by Otsu. The bimodal histogram is a representation of the distribution of pixel intensities in the image. In this case, the threshold will be determined by analysing the histogram. It's predicated on the paradoxical idea of increasing intra-class variance in order to decrease inter-class variance. The global threshold provides satisfactory outcomes if the image's background is relatively consistent. More frequent changes in background intensity may be better handled by adaptive thresholding (also called local or dynamic thresholding). When compared to global thresholding, local thresholding is extremely sluggish.

b. Multi-Otsu Thresholding**:** When applied to an input image, the multi-Otsu threshold divides pixels into multiple classes based on the relative intensity of grayscale tones.

b. Watershed segmentation: The watershed method uses grayscale picture brightness to define two sections. Brilliant pixels create a landscape with a high peak. Markers flood the terrain until flood basins converge at peaks. Basins are distinct regions. Regular regions can be compacted.

c. Region-based RAG: A graph representing the adjacency of regions, known as a "region adjacency graph," is the input to this algorithm. Each area constitutes a "node" in the graph. When comparing the two halves, the average colour difference between them will be used to determine how much weight to give to the edge between the two sections.
d. Felzenszwalb Segmentation: Minimal spanning tree-based grouping segments multichannel pictures (RGB image). The Gaussian kernel refines the image before segmentation. User choices are offered. Colour space pixels' Euclidean distance is used.
e. SLIC - K-Means based image segmentation**:** As with the quick shift technique, Specifically, it employs the K-means method on the 5d colour-and-position space of images. In addition to being efficient, it's also very user-friendly. It's up to the user to supply multiple individual pieces.
f. Quick shift image segmentation: This approach to image segmentation uses local mode-seeking algorithms, which are effective for 2D images. Multi-scale hierarchical segmentation is performed simultaneously. The approximate local density is shown on this scale. Altering the level also allows for hierarchical partitioning. Table (3.1) provides an illustration of the differences between several of these methods.

Table 3.1: Distinctions in Segmentation Methods.

Method	Description	Advantages	Disadvantages
Thresholding	Use histogram peaks	It's the one that doesn't call for any prior knowledge and can be executed with minimal effort right away	Extremely peak-dependent, but ignores spatial detail
Edge-based method	Use discontinuity detection	Low background noise; clearly distinguishable similarities	Inadequate for pictures that have too many frame edges.
Region based	Use partitioning image	There isn't a lot of background noise, and the similarities are clear.	Very costly procedure
Clustering	Use homogeneous clusters divisions	Helpful in avoiding the core issue	Function membership is difficult to define.
Watershed Method	Use topological interpretation	Stables	Gradient computations can be complex.

3.3.1 Thresholding in Image Segmentation

Regarding strategies for partitioning images, thresholding proves to be the most rudimentary and prevalent. Its application enhances distinguishability between objects situated in the foreground versus those located in the background. Although elements reserved into a single category via this technique will exhibit congruent values, they are unlikely to congregate together as one cohesive unit. The identification of air pockets amidst soil samples should not present any cause for alarm since it does not affect depiction either from a two-dimensional or three-dimensional context. In disparate instances, subcategorization based on interrelated regions would entail incorporating thresholding methodology as an additional filtration tool within the already established primary categorizations [75].

3.3.1.1 Bi-level thresholding (BT)

Binarization's goal is to classify pixels as either foreground or background, with the former having a constant intensity and the latter receiving a variable intensity. During image thresholding, an input image (f) is segmented into a binary output image (g).

$$g(i.j) = 1 \; for \; f(i.j) \geq th \qquad (3.1)$$
$$g(i.j) = 0 \; for \; f(i.j) < th$$

where th is the thresholding, g(i, j) is 1 for object image elements, and g(i, j) is 0 for background image elements. If there is no overlap between the objects and the Gray levels of the objects and the background are easily distinguishable, thresholding is a good segmentation method to use. The proper threshold must be selected for threshold segmentation to be effective. A threshold detection algorithm or real-time processing can reach this conclusion. The thresholding technique has the limitation of producing only two classes and being ineffective with multichannel images [76].

3.3.1.2 Multilevel thresholding (MT)

In thresholding, pixels in a grayscale image are categorized according to their intensity levels (L). This classification necessitates the selection of a threshold value (th) and the application of the basic rule of:

$$C_1 \leftarrow p\ if\ 0 \leq p < th \tag{3.2}$$

$$C_2 \leftarrow p\ if\ th \leq p < L-1$$

where p denotes one of the $m \times n$ pixels of the grayscale image g that can be rendered in L grayscale levels. L = 0, 1, 2, ..., L - 1. The classes in which the pixel p can be found are C_1 and C_2, respectively, and the threshold is th. Eq. (3.2) is a bi-level thresholding rule that can be simply extended for numerous sets of data.

$$\begin{aligned} C_1 &\leftarrow p\ if\ 0 \leq p < th_1 \\ C_2 &\leftarrow p\ if\ th_1 \leq p < th_2 \\ C_{i+1} &\leftarrow p\ if\ th_i \leq p < th_{i+1} \\ C_n &\leftarrow p\ if\ th_k \leq p < L-1 \end{aligned} \tag{3.3}$$

Different thresholds are represented by th_1, th_2,..., th_i, th_{i+1}, th_k. Both bi-level and MT have the difficulty of selecting the th values that accurately identify the classes [30][72].

3.4 OTSU MULTILEVEL THRESHOLDING

First proposed in 1979 by Nobuyuki Otsu, the Nobuyuki Otsu algorithm belongs to the global thresholding type of algorithms. One reason why the Otsu method is so popular is that it is a simple yet effective way to segment images based on their maximum variance values. Then it comes to automatic image thresholding, Otsu's approach uses a histogram-based strategy that's surprisingly easy to implement. According to Otsu's algorithm, the image can be classified into two major categories: There are two types of backgrounds: 1) foreground and 2) backdrop. To partition the histogram into two segments, the algorithm endeavours to discover a threshold value that minimizes the combined dispersion while maximizing the "between class variance." The multi-Otsu thresholding method extends the capabilities of the initial Otsu's technique by introducing supplementary thresholds. This approach amplifies its functionality in image segmentation and analysis [40], [77]. To perform image segmentation, Otsu presented a nonparametric approach for thresholding that considers the maximum variance among different classes. By examining the L intensity levels in a

grayscale image, it becomes feasible to determine the probability distribution of its intensity values [24]:

$$ph_i^c = \frac{h_i^c}{N}\ ,\ \sum_{i=1}^{N} ph_i^c = 1 \tag{3.4}$$

$c = \left\{ \begin{matrix} 1.2.3.\ \text{if RGB.} \\ 1.\ \text{if grayscale} \end{matrix} \right\}$ where:

ph_i^c = Distribution probability

h_i^c = Pixel value corresponding to the intensity level from i until c

N = the number of pixels in the image

I = intensity level ($0 \leq i \leq L\text{-}1$)

C = Image component (grayscale or RGB)

The subsequent phase of the histogram entails standardizing it through a probability distribution procedure, which involves utilizing equation (3.5):

$$w_0^c(th) = \sum_{i=1}^{th} ph_i^c\ ,\ w_1^c(th) = \sum_{i=th+1}^{th} ph_i^c\ . \tag{3.5}$$

$$C_1 = \frac{ph_1^c}{w_0^c(th)}, \ldots, \frac{ph_{th}^c}{w_0^c(th)}, C_2 = \frac{ph_{th+1}^c}{w_1^c(th)}, \ldots, \frac{ph_L^c}{w_1^c(th)}$$

Where: $\omega 0\ (th)$ and $\omega 1\ (th)$ = Distribution probability from C1 and C2.

Next, use the following equation (3.6) to compute average levels and variations between classes:

$$\mu_0^c(th) = \sum_{i=1}^{th} \frac{iph_1^c}{w_0^c(th)}, \mu_1^c(th) = \sum_{i=th+1}^{th} \frac{iph_1^c}{w_0^c(th)}\ , \tag{3.6}$$

$$\sigma^{2^c} = \sigma_1^c + \sigma_2^c, \sigma_1^c = w_0^c(\mu_0^c + \mu_T^c)^2, \sigma_2^c = w_1^c(\mu_1^c + \mu_T^c)^2,$$

Where:

μ_0^c and μ_1^c : average rate for class variants 1 and 2

σ^{2^c}: variants between classes,

σ_1^c and σ_2^c: class variants 1 and 2

The goal function, on the other hand, can be calculated as follows using equation (3.7):

$$J(th) = \max\left(\sigma^{2^c}(th)\right).\ 0 \le th_i \le L - 1,\ i = 1,2, \ldots, k \tag{3.7}$$

Where:

$th = th_1, th_2, \ldots, th_{k-1}$ is a vector that contains multiple thresholds.

3.4.1 Medical Image Segmentation

Segmenting human organs, soft tissues, and sick bodies in three dimensions utilizing computer technology for image processing is referred to in the medical field as medical image segmentation. It does this by separating the image into numerous different sections based on their relative similarity or dissimilarity. With this equipment, doctors can analyze lesions and other regions of interest qualitatively or quantitatively. Therefore, this technology has the potential to greatly enhance the precision and dependability of medical diagnosis. The majority of this variety is now represented by objects made up of cellular representations of tissues and organs[5]. In order to segment a medical image, the procedure goes through the following steps[29]:

a. Acquire a medical imaging dataset including a training set, validation set, and test set. As with many other applications of machine learning, image processing data is often segmented into three subsets. Network models are trained on the training set, verified models have their hyper parameters tweaked on the verification set, and tested models are validated on the test set.
b. Pre-processing and image extension, which typically involves input image standardization, random rotation, and scaling, are used to expand the dataset.
c. Apply the appropriate medical image segmentation technique and then output the resulting segmented images.
d. Performance evaluation of the estimation method. For the purpose of determining whether or not medical image segmentation was successful, it is necessary to develop efficient performance metrics. This is an essential part of the process that needs to be completed.

3.5 ARTIFICIAL SWARM INTELLIGENCE (ASI)

The utilization of Artificial Swarm Intelligence technology has been found to enhance the forward-looking abilities of interconnected human organizations by boosting their collective perspectives. AI algorithms that scrutinize the actions and arrangements of natural swarms inform real-time systems, which synchronize web-based user groups. The performance of looped entities like hive brains and human swarms is different from that of conventional approaches for exploiting group expertise. Swarming permits a community to think cohesively and converge on optimal solutions as one unified intellect - an approach unlike voting, polling, surveys or prediction markets requiring every individual in isolation providing data for statistical amalgamation purposes [78][79]. ASI systems employ algorithms that mimic the way nature works by drawing inspiration from the ideas behind Swarm Intelligence. Flocks of birds, schools of fish, and colonies of bees all benefit significantly from this phenomenon when they work together as a single super-organism. With the help of ASI, distributed teams of humans can work together in real time to find optimal solutions to problems that take into account everyone's unique set of expertise, perspectives, and experiences. Unlike elections, polls, surveys, and markets, which rely on large samples sizes to produce meaningful results, "human swarms" can produce meaningful results with much smaller populations because participants act, respond, and engage, constantly altering their conviction as the group converges [80].

3.5.1 Black Widow Optimization Algorithm (BWO)

To enhance engineering design, a new population metaheuristic algorithm called the BWO has been introduced. Black widow spiders have an unusual mating ritual that includes a stage of cannibalism, and this is essentially what inspired the BWO process. With its involved operators, the BWO can be classified as an evolutionary algorithm (EA). Similarities between BWO and GA in their component structures suggest an important evolutionary process is at work. The BWO is strikingly similar to the process of natural evolution in comparison to other EA, especially in terms of the three most crucial aspects of that process: selection, reproduction, and mutation [81]. These parameters distinguish one EA from another because of their unique characteristics. But BWO have taken the weird breeding techniques of black widow spiders and run with it. However, this algorithm deviates in a few

key ways from standard EA, and these differences aid in the algorithm's ability to analyse complex problems more thoroughly. Darwin's theory of natural selection, which proposes that species undergo gradual change over time, leading to the emergence of new species, served as inspiration for the BWO method. The BWO method is well suited to solving optimization problems with multiple local optima, as it keeps the exploration and exploitation phases in equilibrium while still providing rapid convergence[82].

Black widow spider mating behaviour inspired this algorithm. The redback spider, or Australian Black Widow, lives in dry South and Western Australia. This spider lives in Australia, Southeast Asia, and New Zealand. Adult female spiders tower over males. Female spiders can reach 10 mm, but male spiders rarely exceed 4 mm. A red stripe runs across the adult female spider's abdomen. Female adult spiders have red stripes on their top abdomens. Sexual cannibalism occurs when female black widow spiders eat males. Sexual cannibalism occurs when females feed males before, during, or after mating. The mature female black widow spider marked her territory by spraying pheromone hormone on her web. This pheromone attracts male spiders to traps [83]. In order to attract male spiders to a trap, this pheromone can be used as a scent. The female spider will then use her two front teeth to pounce on the male spider and inject a highly lethal poison into its victims. Afterward, the female spider will encase the male in silk and drain his fluids. Therefore, the process will not conclude here because cannibalism will persist among spiderlings. Sibling It is commonly referred to as cannibalism. The young spiders will live in the mother's web and eat each other before being carried away by the wind. There is no doubt that this action will have repercussions on the population, but bolstering parental fitness is helpful because it increases the likelihood that offspring will be born in healthy bodies. Finally, it has been reported that sometimes unfertilized spiderlings slowly consume their mothers. This practice, known as "matriphagy," refers to the consumption of maternal organisms. As a result, a number of variables contributed to all of these cannibalistic behaviours[84][85],

a. Competing against one another.
b. There is a scarcity of food.

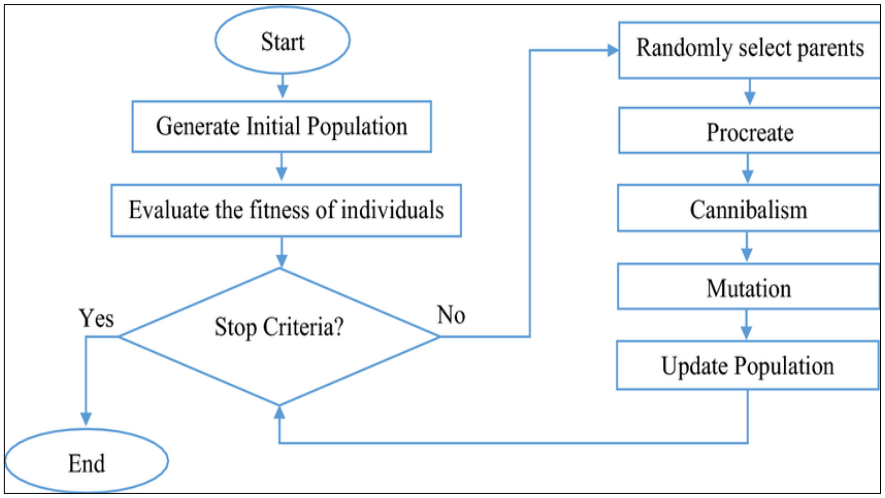

Figure 3.2: Flowchart of the Black Widow Optimization Algorithm [84].

a. Steps in BWO Algorithm:

This section presents the basic steps of the Widow Optimization Algorithm (BWO):

a. Initial population: It is necessary to provide a consistent framework for the many outcomes of the problem variables in order to find the optimal solution. This structure is referred to as a "chromosome" in GA and PSO but a "widow" in black widow optimization. Black Widow Optimization Algorithm envisions several options for solving a problem as Black Widow spiders. The problem's parameters are represented by the Black widow spiders.

$$\text{Widow} = [x_1 , x_2, \ldots, x_{Nvar}] \tag{3.8}$$

Each of the variable values ($x_1 , x_2, \ldots, x_{N_{var}}$) is floating-point number. The fitness of widow is obtained by evaluation of fitness function f at a widow of ($x_1 , x_2, \ldots, x_{N_{var}}$).

$$\text{Fitness} = f(\text{widow}) = f(x_1 , x_2, \ldots, x_{N_{var}}) \tag{3.9}$$

A candidate widow matrix of size $N_{pop} \times N_{var}$ is produced with an initial population of spiders to begin the optimization method. The mating phase, in which the male black widow is eaten by the female either during or after the act of procreation, is then carried out by randomly selected sets of parents [86].

b. Procreate: A candidate widow matrix of size $N_{pop} \times N_{var}$ is produced with an initial population of spiders to begin the optimization method. The next step, reproduction, is carried out by unplanned sets of parents in which the male black widow is eaten by the

female black widow either during or immediately after mating. If the widow array has random values, then an array named alpha must be established, and offspring are generated by applying the following Eq. (3.10) in which x_1 and x_2 are parents, and y_1 and y_2 are offspring.

$$\begin{Bmatrix} y_1 = \alpha \times x_1 + (1 - \alpha) \times x_2 \\ y_2 = \alpha \times x_2 + (1 - \alpha) \times x_1 \end{Bmatrix} \quad (3.10)$$

This method is done $N_{var}/2$ times, with the exception that the numbers chosen at random should not be duplicated. A final step involves sorting the mother and offspring into an array according to their fitness values, with the highest-scoring cannibals being added to the newly formed population. Pairings must adhere to these guidelines [87].

a. Cannibalism: Black widow females are notorious for sexually cannibalizing their mates, either during or after mating. It's possible to tell men from women by looking at their fitness levels, thanks to this method. The stronger spiderlings will eat their weaker siblings, a behaviour known as sibling cannibalism. The number of survivors is determined by the algorithm, so give it a cannibalism rating (CR). Spiderlings regularly engage in the third form of cannibalism, which sees them devouring their mothers. Young spiders' fitness levels were used to classify their overall health and potential[87].

b. Mutation: The subsequent action of Mute pop involves randomly selecting individuals from the population. The optimal scenarios involve the random interchange of two components within the array, as depicted in Figure (3.3).

The mutation rate plays a crucial role in determining mute pop's formation [88].

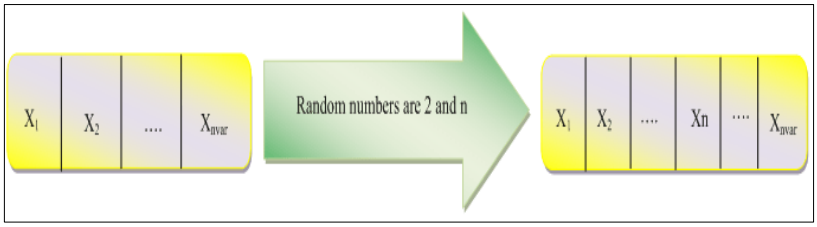

Figure 3.3: Mutation[88] .

c. Convergence: It is possible to take into account three-stop conditions, much like with other evolutionary algorithms [88]:

a. There is a set limit on the number of iterations.

b. After a number of cycles, it was discovered that the best widow's fitness value had not changed.

c. Obtaining the level of accuracy that is required.

The paragraphs that follow, will demonstrate how BWO can be utilized to solve a number of different benchmark optimization challenges. Because the optimal solutions to benchmark functions are known in advance, the accuracy level of experimental algorithms can be determined by reaching a present level of performance. This is because the ideal solutions to benchmark functions are known in advance [88].

d. Parameter setting: To enhance the performance of the proposed BWO algorithm, specific values need to be assigned for its parameters. These include variables such as reproduction speed, cannibalism frequency, and mutation occurrence rate. By configuring the algorithm's settings accordingly, it is possible to improve its effectiveness in identifying optimal solutions. Additionally, further fine-tuning of other parameters can help increase chances of avoiding local optima's and exploring a wider search space globally. It is crucial to meticulously select suitable parameter values that ensure equilibrium between exploration and exploitation stages enabling optimum outcomes. The fundamental building blocks of the BWO algorithms' behaviour rely on three main variables namely peak power, peak current &peak memory levels which are pivotal towards attaining desirable results through this technique:

The term "procreation proportion" (PP) refers to the ideal number of people who should have children. Through controlling the generation of offspring with varying characteristics, this parameter increases diversity and enables more thorough exploration of the search space.

The parameter CR determines how the cannibalism operator behaves, which in turn determines which members of the population are eliminated. Finding the value that is best for this parameter enables peak performance to be achieved during the exploitation phase. This is accomplished by transferring the search agents from the local to the global stage and back again. The PM measures the participation rate in mutation. Finding a happy medium between the exploiting and exploring phases requires setting this parameter correctly. Using this variable, you can steer search agents toward the best possible solution and control their transition from the global to local search phase [88].

b. Applications of BWO Algorithm:

There are many different engineering optimization problems that can be tackled with the help of the BWO algorithm, including [87]:

a. Feature selection.

b. Information retrieval.

c. Text clustering.

d. Hybrid clustering analysis.

e. Text document clustering analysis.

f. Document clustering.

g. Clustering techniques.

h. Cloud computing optimization in IoT, and so forth.

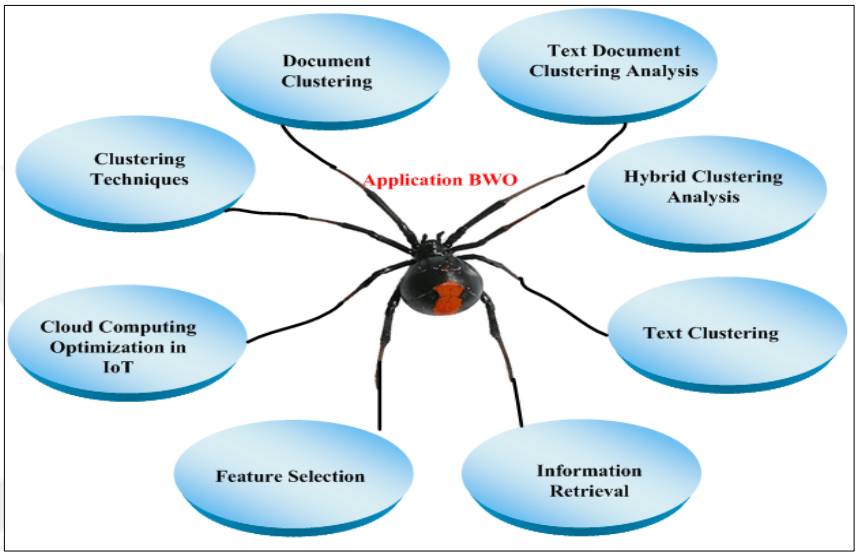

Figure 3.4: Applications of BWO Algorithm.

c. Advantages and Disadvantages of BWO:

Here, Table (3.2) presents some of Advantages and Disadvantages of BWO as follows[82]:

Table 3.2: Advantages and Disadvantages of BWO.

Advantages	**Disadvantages**
Better results in the exploration and exploitation phases.	New optimization algorithm
Produce a rapid rate of convergence.	Does not fully exposed yet.
Capable of sweeping a wide region for optimal solutions.	

Cryptographic Algorithms: Information sent between parties in different locations can be kept secure through the use of cryptography. Encryption is the first step in the process, but the data is meaningless until it is decrypted [89][90]. Since the invention of computers, storing, processing, and retrieving data have become much easier tasks. Nearly everyone, from individuals to government agencies to the courts to businesses of all sizes, makes use of internet-based computers and services. Professionals in information security and computer scientists have their work cut out for them because cybercriminals are just as quick to adopt new technologies [91]. Modern technology may be simple and intuitive, but it also presents some risks. In this room, everyone is overjoyed by the convenience of their laptops and smartphones. Various online applications, such as social media sites, retail and banking websites, and more, are available to users at any time of the day or night. In contrast, if a hacker obtains access to a user's banking password, he or she can steal funds just as easily. Someone else could potentially hack into your social media accounts and use your information for bad. Therefore, it is of the utmost importance to safeguard information as it resides in applications, travels across networks, and is stored on computers [92][93].

The safest way to prevent unauthorized parties from accessing sensitive information is to encrypt it. Making it difficult to intercept data is a central principle in the design of cyber defences. It's not just government secrets that can benefit from this idea; any sensitive data can be safeguarded in the same way. Asymmetric and symmetric cryptography are the two main types of security protocols. Symmetric encryption relies on a single secret key for both sending and receiving, while asymmetric encryption calls for two keys to be kept track of by the sender and receiver [94][95]. Academically paraphrased text the symmetric cryptography methods, including DES, 3DES, CAST-128, BLOWFISH, IDEA, AES and RC2/RC6 employ a single key for both encryption and decryption. Conversely, asymmetric algorithms or public-key systems such as SSH, DH, DSA, RSA and SSL/TLS operate with two different keys: the public and private. Notably demonstrated in Figure 3.5 are specific instances where each process requires a separate key to function efficiently [96].

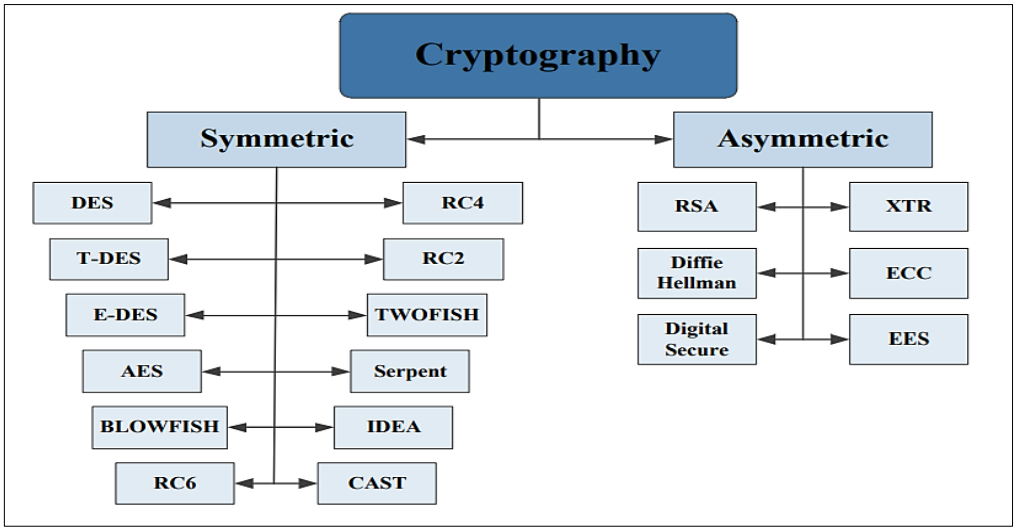

Figure 3.5: The Classification of Encryption Algorithms [96].

3.5.1 Advanced Encryption Standard (AES)

This method was suggested as a replacement for DES by NIST in 2001. AES is capable of providing any number of databases. When AES algorithm is employed for encryption and decryption with 128-bit keys, it undergoes ten rounds of encoding and decoding. For 192-bit keys, the encrypted message should be transmitted after twelve complete cycles of encoding while in case of a 256-bit key, fourteen such cycles are required before transmitting the resultant encoded message. The maximum data length supported by AES is up to 128 bits which can be fragmented into four autonomous working blocks that are consolidated as one byte line. This amalgamated state matrix comprises a square arrangement consisting of sixteen bytes packed together in four rows and columns each respectively yielding a dimensionality size equalling four-by-four (4x4) [97].First, the "Add round key stage" is used to encode and decode data. However, the output undergoes nine basic rounds, each of which comprises four modifications, before the final round: Sub-bytes, Shift-rows, Mix-columns, and Round-Key addition are the first four operations. The eighth-round lacks access to the mix columns transformation. Figure summarizes the entire process (3.6). Instead, then encrypting data, decryption involves the inverse procedure, consisting of the following steps [98]:

a. Substitute Byte Transformation*:* Data blocks in AES are 128 bits in length, so each record in a database will take up 16 bytes. Rijndael s-boxes, 8-bit substitution boxes, are used in sub-byte transformation to change each byte of a data item into a different byte.

b. Shift Rows Transformation**:** This is a simple transformation, which cycles the bytes in the state's final three lines that are sensitive to row order. On the second line, we perform a left-to-right byte shift. In the third and fourth rows, there were circular shifts of two and three bytes, respectively.

c. Mix Columns Transformation: This set is the complement of a set that multiplies the columns of all the states by themselves. An unchanging matrix is multiplied by each. In this process, bytes are handled like a list of different names.

d. Round Key Transformation: An XOR operation between the 128-bit round key and the 128-bit current state. The opposite of this is transformation.

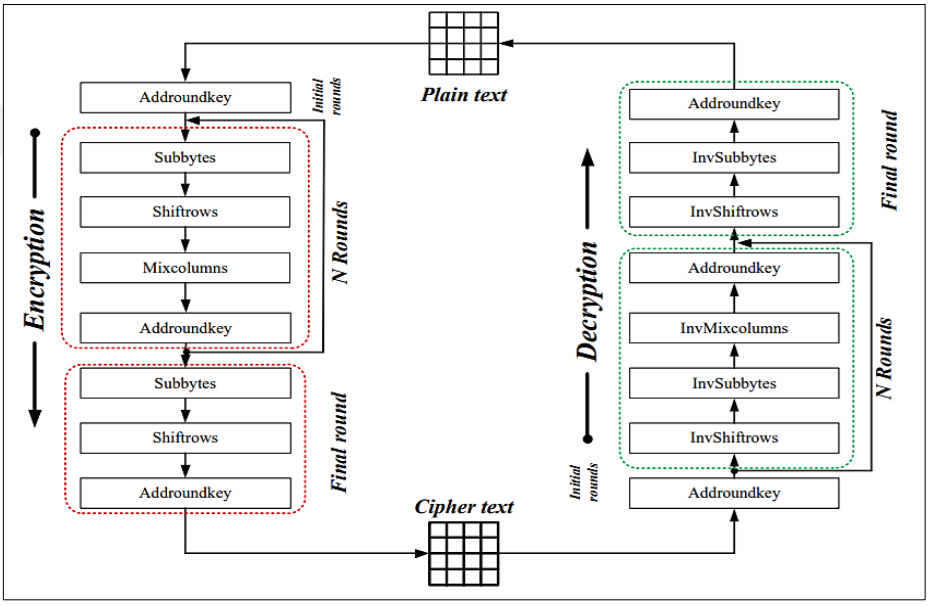

Figure 3.6: Advanced Encryption Standard Process [98].

Quality Measurement Techniques: Many different methods exist for measuring and evaluating image quality, including Mean Square Error (MSE), Peak Signal to Noise Ratio (PSNR), Structured Similarity Index Method (SSIM), and Standard Deviation (SD) [99]as follows:

a. MSE (Mean Square Error)

Measured standard error (MSE) is the most popular metric for estimating image quality. Since it's meant to be an all-encompassing reference metric, a lower value is preferable. It's the second time this mistake has happened. Mean squared error incorporates the bias and variance of the estimator. The MSE is equal to the variance of the estimator if it is unbiased. Measured in the same units as the square of the quantity being calculated, in this instance

variance. Mean Squared Error (MSE) between two images such as $g(x.y)$ and $g^{\wedge}(x.y)$ is defined as Eq. (3.11):

$$MSE = \frac{1}{MN}\sum_{n=0}^{M} \sum_{m=1}^{N}[\, g^{\wedge}(n.m) - g(n.m)]^2 \tag{3.11}$$

b. PSNR (Peak Signal to Noise Ratio)

The PSNR is an acronym for signal-to-noise ratio, which represents the proportional measure of maximum signal power to noise contamination. This index provides a quantitative assessment of how effectively the given signals counterbalance undesired effects during transmission or representation. The disparity between two visual inputs can also be estimated in decibels using logarithmic notation as it encompasses wide variations presenting sufficient resolution dynamics ranging from minimum to maximum quality levels. In particular, when determining the probable reconstruction accuracy concerning lossy image compression codecs, peak signal-to-noise ratio serves as benchmarking criterion preferred by researchers and practitioners alike due to its reliability in approximating results that match human perception experiencing superior standards through codec outputs. The calculation involves deriving the quotient value after dividing variance components comprising distortion caused by error-prone procedures that transform original-untainted data producing unwanted artifacts affecting clarity with constant amplitude-based random fluctuations reflected through noisy channels discouraging optimal reception fidelity.

$$\text{PSNR} = 10\ log_{10}\ (peakval^2)/\text{MSE} \tag{3.12}$$

The highest point in the picture data is referred to as the Peak Val (Peak Value). Unsigned 8-bit integers can only go as high as 255.

c. Structure Similarity Index Method (SSIM)

One such perceptual-based model is the Structural Similarity Index Method. In this technique, the perception of structural information shifts constitutes image degradation. This applies not only to luminance masking and contrast masking, but also to other essential perceptual truths. The term "structural information" is used to describe the relationships between and confinement of pixels that have strong dependencies on one another. These tightly dependent pixels in the image domain denote some additional crucial data about the objects being viewed. The term "luminosity masking" describes the method used to reduce

the visibility of distortion at the image's periphery. Contrast masking, on the other hand, is used to cover up flaws in an image's texture. The SSIM measures how clear an image or video appears to be to the viewer. It measures the degree of similarity between the original and the restored image. The formula for SSIM is:

$$SSIM\ (x.y) = \ [l(x.y)]^{\alpha} \cdot [c(x.y)]^{\beta} \cdot [s(x.y)]^{\gamma} \tag{3.13}$$

d. Standard Deviation (STD)

In the fields of probability and statistics, it is a standard technique for measuring dissimilarities. Indicates the degree of variation from the norm (mean). Data points with a big standard deviation have values that are all over the place, while data points with a small standard deviation have values that are concentrated close to the mean. For every given collection of data, statistical population, or probability distribution, simply finding the square root of the variance yields the standard deviation. The variance of a set of numbers is the average squared difference (standard deviation) between each number and the mean. This metric is simpler to calculate than the average absolute deviation, but it is not as accurate. Unlike variance, which is often expressed in a different unit system, the Standard Deviation (STD) is always expressed in the same units as the data. The sample standard deviation and mean are displayed in each diagram as (3.14). (3.15).

$$\text{Standard Deviation (STD)} = \ \sigma = \frac{1}{n}\sum_{i=1}^{n}(X_i - \bar{M})^2 \tag{3.14}$$

Where: (n) =can be defined as the number of samples in each of the frames.

X_i =can be defined as the value of the signal.

$\bar{M}$= Mean the sample of the signal.

$$\bar{M} = Mean = \ \frac{1}{n}\ \sum_{i=1}^{n}(X_i) \tag{3.15}$$

e. Unified Average Changing Intensity (UACI)

The closer UACI approaches 33.333 percent, the more secure a cryptosystem is against differential attacks. The UACI algorithm calculates a mean difference intensity between the plain and encrypted pictures. The following equations [100] are used to derive those two measurements:

$$\text{UACI} = \frac{1}{\text{Width}\times\text{Height}}\Sigma_{\text{i,j}}\left(\frac{\text{C}_1(\text{i,j})\text{XC}_2(\text{i,j})}{255}\right) \times 100\% \tag{3.16}$$

The encrypted image before the change of a single pixel in the original plain image is denoted by c1(i, j), and the encrypted image after the change by c2(i, j).

f. Information Entropy

Cryptography relies on randomness to prevent information theft. Randomization must be present. One interpretation of entropy is that it quantifies randomness. It determines data trustworthiness. We need security algorithms that can generate a lot of randomness for encrypted messages to protect confidential data. As a result, the key and ciphertext depend less or not at all. The key-ciphertext connection is complicated by system noise. This trait is sometimes called confusion. To prevent an attacker from making educated guesses, confusion is ideal. It'll be harder for the attacker. Cryptographic performance is measured by entropy. Encryption algorithms protect data [27], [101] . The following formula can be used to represent the entropy of image data:

$$H(m) = \sum_{i=0}^{2N-1} p(m_i) \log_2 \frac{1}{P(m_i)} \tag{3.17}$$

4. METHDOLOGY

4.1 INTRODUCTION

To create a practical multilevel segmentation approach that approximates the solution to the normalized cut segmentation problem, we introduce the Segmentation by Otsu algorithm. Make a powerful segmentation strategy with the use of metaheuristic algorithms like the BWO Algorithm. These algorithms can determine, in a reasonable amount of time, what thresholds are best suited for a given image. Some of the first attempts at developing a quick multilevel segmentation system relied solely on pixel intensity to create their segmented images. More low- and high-level visual signals were introduced to produce stronger contrast between two locations, allowing for more accurate segmentation of more complex images. This was implemented in improved versions of the program. Better results were achieved with the BWO method by factoring in regional features such pixel intensity variance and form moments of clusters of pixels. The prosed algorithm and its constituent parts are laid out in this chapter.

4.2 PROPOSED SYSTEM

a. Thresholding Phase

Thresholding is a common approach for finding and separating edges in images. Using a histogram diagram of the image, we search for thresholds that allow for clear separation of image boundaries and borders and that help to minimize the overall number of brightness levels. These thresholds are helpful in reducing the overall number of brightness levels. A more comprehensible picture is shown when the objects' borders are well delineated. Figure (4.1) shows how a histogram can be used to locate the best possible threshold for an image.

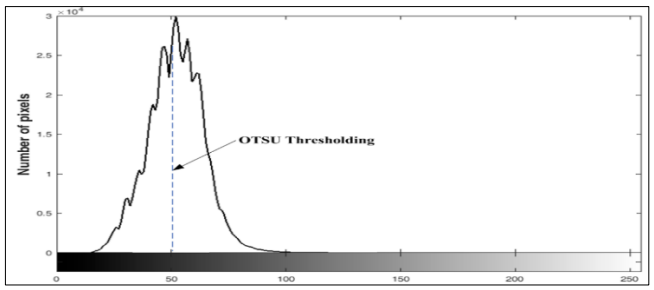

Figure 4.1: Optimal Threshold by Otsu Threshold**.**

Here, a threshold has been set to a value of 50, so that areas of the image with illuminances below that threshold are shaded and those above it are seen in their full brilliance. The key issue is determining how much this threshold should be for optimal visual quality in the final output image. This issue can be addressed with the use of threshold approaches, which can determine the best threshold to utilize. When it comes to thresholding images, Otsu thresholding is a powerful and widely used technique that may be used to isolate foreground elements from their surrounding backdrop.

Otsu thresholding's runtime and complexity are manageable for one or more thresholds, but they increase with more thresholds. Otsu Thresholding uses statistical methods to establish reasonable thresholds. The optimal values are calculated by taking the difference between the median and the standard deviation of the light levels on either side of the thresholds. The method uses a recursive process, as shown in Figure (4.2), to establish the thresholds:

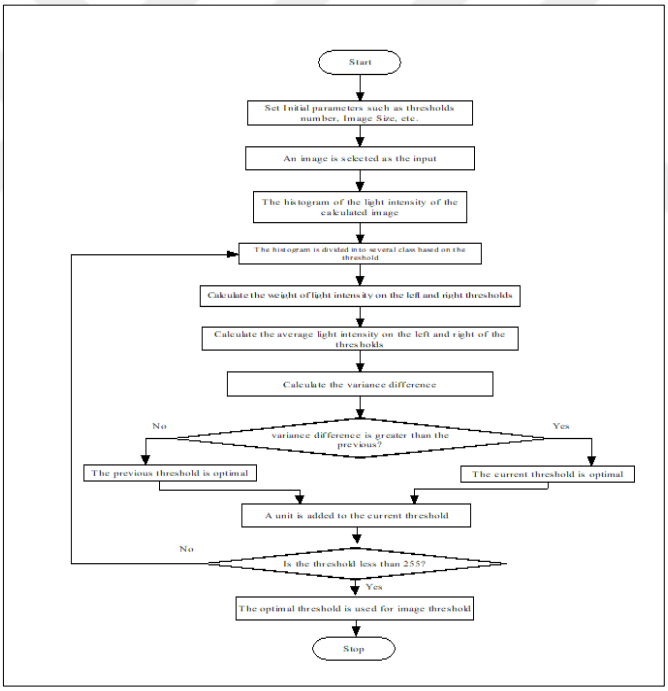

Figure 4.2: Otsu Thresholding.

The Otsu thresholding method is an absolute approach that may be used to determine when a photograph has passed a particular threshold. The algorithm that underpins this method works to optimize the light intensity variance on both sides of the thresholds. The following phases make up the Otsu thresholding method, and the ones that follow are an attempt to streamline the process by employing the black widow optimization algorithm:

a. To test all 256 levels of sensitivity in a grayscale image, we first apply the minimum amount of light (threshold) by setting the brightness to zero.
b. After determining the average weight of the light intensity of the pixels that are to the left of the threshold, the following step is to figure out the average weight of the pixels themselves.
c. The weighted average dispersion of the subsets on either side of the cut-off is added together.
d. If the estimated objective function value is larger than the optimal threshold, the new optimal threshold is employed.
e. After a thorough evaluation, the best threshold is chosen, and it is put to use classifying the histogram and the image diagram.

In this method, the optimal threshold is identified by first analysing each and every threshold present in the image, which ranges in value from 0 to 255, if the number of thresholds is greater than one and equals n, then 255^n is used as the threshold value. Finding thresholds requires searching through a huge number of states, and this number grows as more thresholds are added. It is hoped that the proposed approach can calculate these many thresholds with a reasonable amount of time and error. During the process of black widow optimization, the proposed method depends on accurately framing the problem, establishing the objective function, and taking into consideration all of the solutions that are practically possible. In the method that has been suggested, the thresholds in the photo histogram diagram, which are determined with the use of Eq. (4.1), show several ways of approaching the issue. Random threshold sets, or "black spiders," are generated as initial solutions for the black widow optimization method, which operates on a brightness scale from 0 to 255.

$$BWO_i = \ll BWO_i^1, BWO_i^2, BWO_i^3, \dots, BWO_i^D \gg \tag{4.1}$$

$$BWO = \begin{matrix} BWO_1^1 & BWO_1^2 & \dots & BWO_1^D \\ BWO_2^1 & BWO_2^2 & \cdots & BWO_2^D \\ \vdots & \vdots & \vdots & \vdots \\ BWO_n^1 & BWO_n^2 & \cdots & BWO_n^D \end{matrix} \tag{4.2}$$

In this relationship, BWO_i is a threshold vector in the image histogram diagram and is considered a member of the BWO algorithm. BWO_i^j is also the j-th threshold of the image

in the i-th member of the proposed algorithm, and also D is the number of thresholds used in the image. Within these associations, BWO represents a set of n thresholds shared by the proposed algorithm's n participants. Each of these thresholds requires a decision from the Otsu goal function. Eq. (4.3) can be used to assess either a threshold set or a spider:

$$f_{Otsu} = w_0(\mu_0 - \mu_T)^2 + w_1(\mu_1 - \mu_T)^2 + .. + w_m(\mu_m - \mu_T)^2 \tag{4.3}$$

The objective function of m is the various thresholds such as vector $\{t_1, t_2, \dots, t_m\}$ for image threshold. With this set of thresholds, the image histogram is divided into m + 1 sections, such as threshold classes $\{C_0, C_1, \dots, C_m\}$ of light intensity. Each threshold set can be sent to the objective function for evaluation, and the value of each spider can be determined using Eq. (4.4). This allows for a population-level evaluation of the proposed approach.

$$f_{Otsu}(BWO) = \begin{matrix} f_{Otsu}(BWO_1^1 & BWO_1^2 & \dots & BWO_1^D) \\ f_{Otsu}(BWO_2^1 & BWO_2^2 & \cdots & BWO_2^D) \\ \vdots & \vdots & \vdots & \vdots \\ \lfloor f_{Otsu}(BWO_n^1 & BWO_n^2 & \cdots & BWO_n^D) \rfloor \end{matrix} = \begin{bmatrix} f_{Otsu}(BWO_1) \\ f_{Otsu}(BWO_2) \\ \dots \\ f_{Otsu}(BWO_n) \end{bmatrix} \tag{4.4}$$

The proposed method begins with the generation of a number of randomly generated thresholds, each of which represents a spider; the range of these thresholds can be thought of as the minimum and greatest light intensity in the photographs, and this light intensity can be thought of as the Eq (4.5):

$$BWO_i^j = L + (U - L).rand(0,1) \tag{4.5}$$

In this context, L and U refer to the lowest and highest possible light intensities in the image, respectively. Rand (0,1) returns a random number between 0 and 1. In step 4.1 of the proposed method, each threshold vector undergoes an application of the algorithm's relations, which causes the value to be updated. For the purpose of establishing the optimal Otsu thresholds, the following processes are carried out by applying the black widow optimization algorithm and the suggested quasi-code:

a. It has been decided upon the parameters of the suggested method, such as the population size and the maximum number of BWO iterations.
b. The proposed approach takes an image as its input.
c. Through the use of pre-processing, the quality of the original image can be improved.
d. This includes determining the image's histogram and the amount of light intensity used most frequently within it.
e. Several of these arrays are created at random from the proposed algorithm's population, which is believed to have a threshold set.
f. The Otsu thresholding objective function has been used to rank each threshold vector and population member in the proposed technique.
g. As the best solution to the proposed approach, a threshold vector with the optimal thresholds is computed.
h. Once a sufficient number of deserving black spiders have been chosen, the population production phase can begin.
i. The image thresholds are utilized to identify two suitable parents from which the combination and blending phase will be based.
j. The cannibalism mechanism is what's responsible for the process of culling the weak population or rejecting the set of thresholds in Otsu thresholding if it doesn't optimize the target function. This is done as part of the Otsu thresholding algorithm.
k. Good populations or adequate thresholds are required for the mutation phase to occur.
l. The proposed algorithm iteratively updates the threshold vectors and recalculates their optimal value.
m. The iteration counter for the method is increased by one, and the stages that came before it is repeated if the counter is still lower than the maximum iteration value; if it is more than that value, the next step is performed instead.
n. Its thresholds the image using the best possible threshold vector.
o. By applying thresholds based on this classification, the input image is separated.

Algorithm (4.1): Black widow optimization(BWO) Algorithm based multilevel thresholding

Input: The test image I

Image pre-processing and normalization length and width of the image

Initialize a population of nPop Spiders with random positions, the number of thresholds m ,MaxIt, rate of procreating, rate of cannibalism, rate of mutation

Compute the image's histogram

Coding thresholds image in the form of a spider:

$$\boldsymbol{BWO_i} = \ll \boldsymbol{BWO_i^1, BWO_i^2, BWO_i^3, \dots, BWO_i^D} \gg$$

Each solution is created in a minimum and maximum random light intensity range:

for i=1** to **n do

for i=1** to **D do

$$\boldsymbol{BWO_i^j = L + (U - L).rand(0,1)}$$

end for

end for

The initial population of black widow spiders: $$\boldsymbol{BWO} = \begin{matrix} \boldsymbol{BWO_1^1} & \boldsymbol{BWO_1^2} & \dots & \boldsymbol{BWO_1^D} \\ \boldsymbol{BWO_2^1} & \boldsymbol{BWO_2^2} & \cdots & \boldsymbol{BWO_2^D} \\ \vdots & \vdots & \vdots & \vdots \\ \boldsymbol{BWO_n^1} & \boldsymbol{BWO_n^2} & \cdots & \boldsymbol{BWO_n^D} \end{matrix}$$

Evaluate each black widow spiders by fitness function:

$$\boldsymbol{f_{Otsu} = w_0(\mu_0 - \mu_T)^2 + w_1(\mu_1 - \mu_T)^2 + .. + w_m(\mu_m - \mu_T)^2}$$

While**(it<=MaxIt) **do

based on procreating rate, calculation the number of reproductions such as "nr'

Select the best nr solutions in pop and save them in pop1

//Procreating and cannibalism

for i=1** to **nr do

randomly select two solutions as parents from pop1:

$\boldsymbol{BWO_j} = \ll \boldsymbol{BWO_j^1, BWO_j^2, BWO_j^3, \ldots, BWO_j^D} \gg$

$\boldsymbol{BWO_k} = \ll \boldsymbol{BWO_k^1, BWO_k^2, BWO_k^3, \ldots, BWO_k^D} \gg$

generate D childern using eq1:

$\boldsymbol{y_1 = \alpha . BWO_j + (1 - \alpha) . BWO_k}$

$\boldsymbol{y_2 = (1 - \alpha) . BWO_j + \alpha . BWO_k}$

destroy father

based on the cannibalism rate, destroy some of children

save the remain solutions into pop2

end for

based on the mutation rate, calculate the number of mutation children such as 'nm'

for i=1** to **nm do

select a solution from pop1

mutate randomly one chromosome of the solution and generate a new solution

save the new one into pop3

end for

//Updating pop

Update pop=pop2+pop3

returning the best solution

it=it+1

end while

return the best solution from pop for image thresholding

Thresholding evaluation with evaluation indicators

4.2.1 Encryption Phase

The process begins with an image that has been segmented. There are three steps involved in this stage, and they occur in the following order:

4.2.1.1 Segment iris image using otsu thresholding

The iris of an eye is usually isolated through segmentation. With the use of multilevel thresholding, we can locate the iris's edge. By fitting two lines with enhanced Otsu thresholding, the eyelids are identified, and the eyelashes are segmented, all utilizing the threshold approach.

4.2.1.2 Optimize segmentation using BWO algorithm

The method used in this study involves the determination of the most favourable threshold value by comparing various thresholds of an image to a number within 0-255 range. The computation becomes more complicated as there is a rise in states required for finding each threshold, making it even more challenging. However, according to our proposed approach, determining numerous criteria can be achieved with satisfactory precision and managed time-frame. To ensure efficient execution of this technique, correct characterization of the issue at hand must be done alongside stating objective function and all feasible solutions appropriately considered to determine solution sets that best fit histogram thresholds using equation (4.1). A probable population-based example utilizing BWO technology resulting in several black spider or intensity patterns between 0 and 255 spans across diverse samples (equation (4.2)). The BWO_i is a threshold vector in the histogram representation of the picture and part of the current procedure. The j^{th} threshold of the image is also the basis for the i^{th} part of the proposed algorithm, therefore $BWO_j = D$, where D is the total number of thresholds in the image. To solve these equations, think of BWO as a population of n thresholds, where n is the number of components in the proposed method. The Otsu objective function must take into account all of these thresholds. You can use eq. (4.3) to examine a spider or a threshold set. The various thresholds are the optimal solution of m such as vector $\{t1, t2, \ldots, tm\}$ for image threshold. The histogram of the image is divided into m + 1 portions. using this set of thresholds, such as threshold classes $\{C0, C1, \ldots, Cm\}$ of light intensity. Each threshold may be used to evaluate the population of the proposed method with the provided objective function, and the value of each spider can be computed with Eq. (4.4). In the first step

of this process, a large number of random thresholds, each of which is a spider, are generated; these thresholds' domain corresponds to the range of values between the lowest and highest levels of sharpness in the photographs' lighting, the latter of which is defined by the Eq. (4.5). Although rand (0,1) is a randomly selected integer between 0 and 1, L and U represent the image's lowest and highest sharpness of lighting, respectively. These threshold vectors are utilized in conjunction with the relations from the proposed method, which cause their values to be updated with each iteration. The steps of the proposed method for determining appropriate Otsu thresholds by means of the BWO algorithm are as follows:

a. Population size and the maximum number of BWO iterations are two of the parameters of a proposed strategy that have been determined.
b. The proposed technique requires an image as input.
c. With proper pre-processing, the quality of the supplied image can be greatly enhanced.
d. The image's histogram is computed, and its sharpness and lighting frequency are identified.
e. The proposed method includes the use of a threshold group, and the corresponding algorithm generates several such arrays as random samples from a larger population.
f. Each threshold vector or population member was graded using the Otsu thresholding objective function.
g. For the given technique, the best thresholds can be found in the optimal threshold vector.
h. Two good parents are selected from the image's boundaries, and their characteristics are blended and combined.
i. Cannibalism is used in Otsu thresholding to eliminate low-density populations or groups of thresholds that do not maximize the objective function.
j. Good populations, or those that have reached the right critical mass, enter a mutation phase.
k. In the proposed method, the threshold vectors are tweaked between iterations, and their optimal value is reassessed each time.
l. If the current number of iterations is less than the maximum number of iterations, the algorithm advances to the next step; otherwise, the previous step is repeated and the iteration counter is increased by one.

The process of encryption is shown in Figure (4.3). Here are the measures used during the encipherment process:

Step 1: The image of the iris was recovered via a thresholding process, and then used to create the binary code.

Step 2: The iris image's binary code is encrypted using advanced encryption standard (AES) to store the user's identifying information.

Step 3: The encrypted data is then saved as ciphertext.

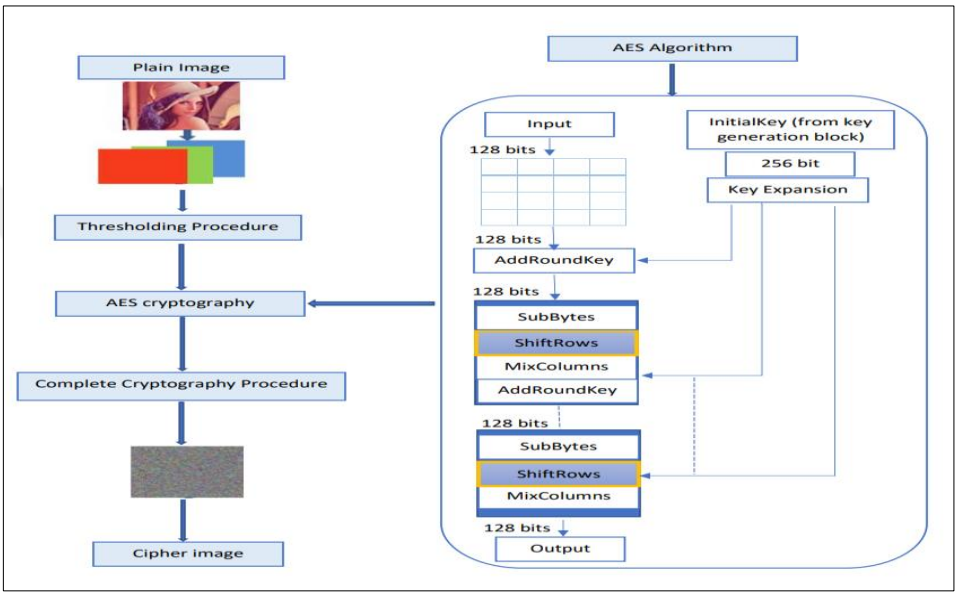

Figure 4.3: AES Encryption Process of the Proposed System.

Figure (4.4) depicts the decryption operation of the proposed approach, with the decryption steps highlighted for clarity. Publicly available iris images will be decoded using AES cryptography in combination with the ciphertext in order to obtain the user identifiers.

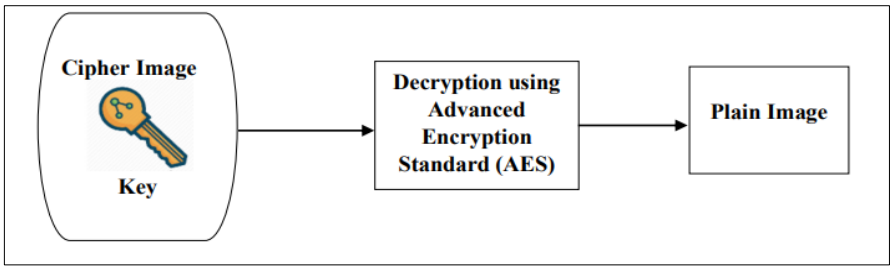

Figure 4.4: AES Decryption Process of the Proposed System.

5. RESULTS

5.1 OVERVIEW

This chapter examines the proposed method for picture thresholding in light of Otsu thresholding. Following an introduction to the threshold standard set of images and the proposed algorithm's evaluation parameters, this article delves into the algorithm's mechanism for thresholding through experiments, before comparing and contrasting the results with those of Otsu thresholding and drawing conclusions about which method is superior.

5.2 DATASET

Otsu thresholding is established using a reference set of photos from this field, allowing the suggested technique to be tested and applied with these images. The suggested algorithm takes as its input a collection of grayscale photographs with a range of light intensities from 0 to 255, as employed in this research. Obtainable from Berkeley's segmentation picture collection, the suggested techniques have been evaluated on a set of six reference grayscale photographs captured by USC. The suggested algorithm can use as its input a collection of photos that have been utilized before in the evaluation of threshold techniques. Several other studies have performed thresholds on these reference images; thus, they can be used to evaluate and compare the proposed approach with other threshold techniques. This study's second section applies the proposed algorithm to the segmentation and diagnosis of brain tumors, using a variety of images of the brain and eyes as training data. Both of these photo sequences are displayed in Figures (5.1) and (5.2) in [24]. The magnetic field's ability to expose the structure of brain tissue is just one of the many ways in which magnetic resonance imaging can be put to use. Segmentation of such images is one method for diagnosing a wide range of neurological disorders, including brain tumours, multiple sclerosis, and Alzheimer's disease. In the medical field, detecting optical discs in retinal pictures is a significant problem that can be handled with threshold and segmentation techniques.

Figure 5.1: Standard Image Set for Evaluating the Proposed Algorithm.

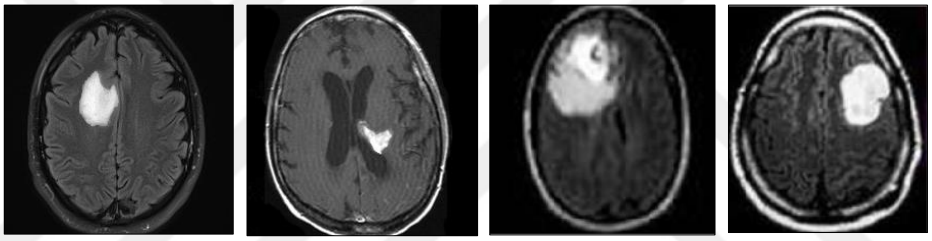

Figure 5.2: Magnetic Resonance Imaging (MRI) set for Evaluating the Proposed Algorithm**.**

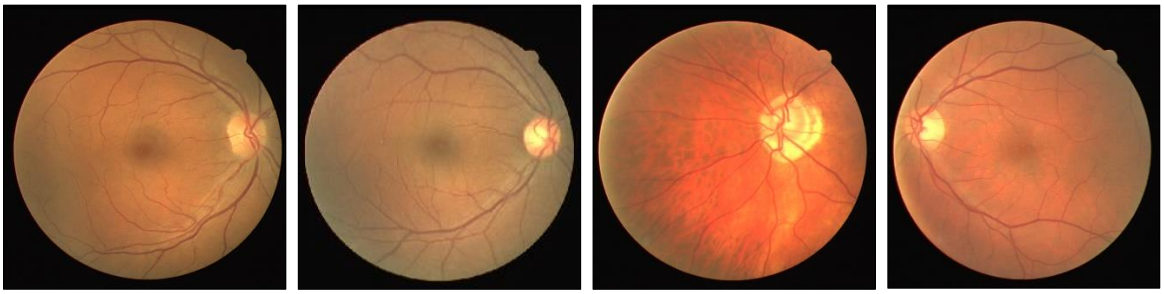

Figure 5.3: Optic Disc Images for Evaluating the Proposed Algorithm.

The dataset used during the secure phase was obtained via a Kaggle download. The Eye Images included in the Multimedia University (MMU1) database can be used to train models of IRIS-based Biometric Attendance Systems. Iris patterns can be used to individually identify individuals. There are 460 photographs in this dataset, including 5 shots of each person's left and right IRIS plus a few blank files. IRIS segmentation can be used to uniquely

identify and classify an IRIS image based on a stable dataset. The photos used in this investigation are shown in Figure (5.4).

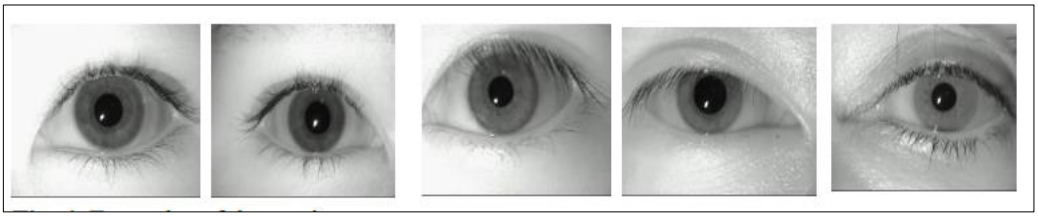

Figure 5.4: Examples of Dataset Images.

5.3 PARAMETERS

To evaluate multi-level thresholds, the proposed approach entails comparing the algorithm with several meta-algorithms through which various methods such as particle swarm optimization, firefly algorithm, symbiotic organisms search, artificial bee colony and gray wolf optimization are assessed. A detailed inventory of parameter values for the different algorithms is presented in Table 5.1 below. To scrutinize the impact that population size and iteration count have on these intended algorithms, variables can be employed.

Table 5.1: Implementation Parameters of the Proposed Method and Other Algorithms.

Algorithm	Parameter	Value	Parameter`	Value
BWO	Procreate rate	0.6	Pm = mutation rate	**0.4**
	CR = cannibalism rate	0.44		
SOS	$BF1$	1	$BF2$	**1**
PSO	c1, c2	2,2	Inertia	**0.6**
ABC	maximum trial limit	0.6		
GA	crossover percentageα	0.9	mutation percentage	**0. 1**
GWO	c	0.01	alpha	**0.1**
	a	[2,0]		

5.4 ANALYSIS OF EXPERIMENTS

This section analyses the proposed algorithm and makes a comparison with established algorithms, namely particle swarm optimization, genetic algorithm, firefly algorithm, symbiotic organisms search, artificial bee colony and Gray wolf optimization. The evaluation criteria include performance metrics such as PSNR, SSIM, time taken for execution and standard deviation based on experimentation.

5.4.1 Qualitative

This research is based on a sample size of 20, and up to 100 repetitions are carried out for the suggested methodology. The current paper employs a model similar to Lena's technique in order to critically examine the advantages and disadvantages of the evaluation procedure. The objective behind these trials was twofold: firstly, they aimed at contrasting our proposed approach with Otsu thresholding method behaviour while exploring an optimal threshold setting by utilizing four equally favourable values (1 through 4). Secondly, as illustrated in Figure (5.5), we implemented Otsu thresholding using thresholds ranging from one-to-four levels on Lena's image experimentally. Further analysis incorporating black widget optimization strategy revealed that our approach effectively competes against Otsu's method across all tested settings with which it consistently showed superior results when applied onto the same Lenas' images used earlier under identical circumstances; this outcome has been depicted in Fig.(5.6).The threshold values calculated by Otsu thresholding and the suggested method are 118 and 118, respectively, as demonstrated in the experiments done on the Lena sample, indicating that there is a difference between the two approaches. They are unrelated to the discovery of a threshold. If there are two thresholds, the Otsu values are 100 and 158, and the suggested approach uses these numbers as estimations. If there are three thresholds, the Otsu threshold approach yields 84, 127, and 169; the suggested method yields 85, 128, and 170; these values differ from the Otsu values by a little margin. The Otsu thresholds were analysed using four different values of 80, 117, 148 and 180. When compared to the computed approach with values of their method at 81,116,147 and179 respectively. Results indicated that the Otsu threshold function proved useful as a target when used in conjunction with proposed iterative methods. The effectiveness of this algorithm for image segmentation was demonstrated by steadily increasing objective

function values over time where higher efficiency correlates with higher objective function value. In Figure (5.7), this pattern is observed through twenty iterations across one hundred repetitions per population based on Camera man insistence results at each of four distinct threshold levels. It is noted how these increases are evident across all tested thresholds during iteration runs suggesting reliable outcomes or repetitive measurements which can support generalizable conclusions regarding optimal performance according to specific image processing goals/goal(s). The increasing value of the objective function over time indicates that the suggested approach is selecting Otsu thresholds with comparable values. To achieve this, the method repeats Otsu's thresholds iteratively until they converge. The effectiveness of this proposed technique was assessed against swarm intelligence-based algorithms such as grey wolf optimization and metaheuristic strategies using genetic algorithm. Other evolutionary techniques including concomitant use of artificial bee colony, symbiotic organisms search, firefly and particle methods were also compared for their utility in improving threshold segmentation performance (1-5) under identical number-of-thresholds conditions within a refined experimental framework designed to test its efficacy.

Otsu, m=1

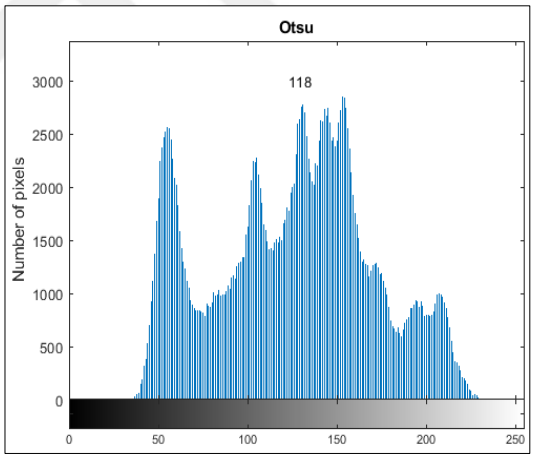

Otsu thresholds: 118

Otsu, m=2

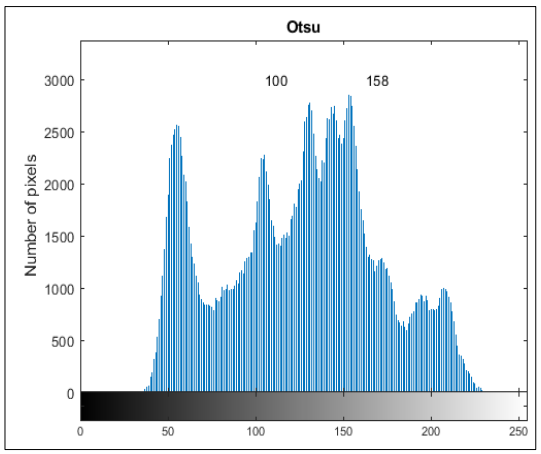

Otsu thresholds:100 and 158

Otsu, m=3

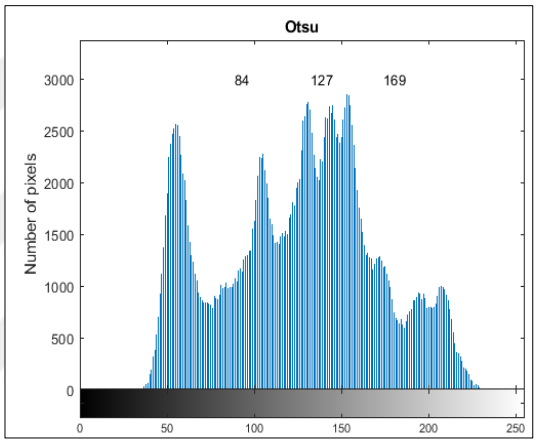

Otsu thresholds: 84, 127 and169

Otsu, m=4

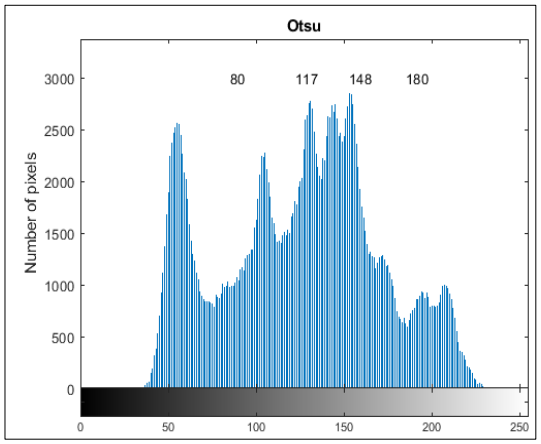

Otsu thresholds: 80, 117, 148 and 180

Figure 5.5: Otsu Implementation on Lena Image.

Otsu, m=1

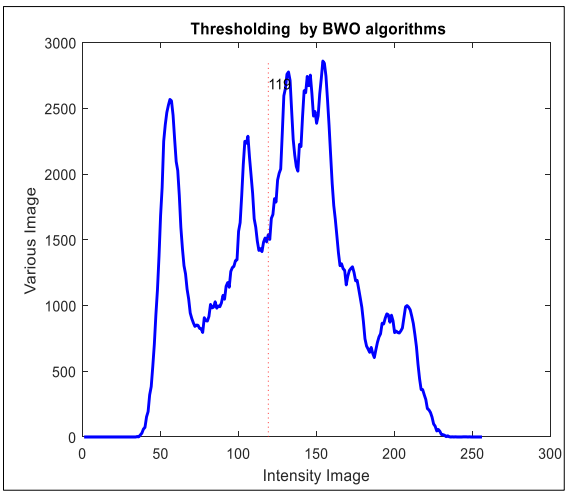

BWO thresholds: 118

Otsu, m=2

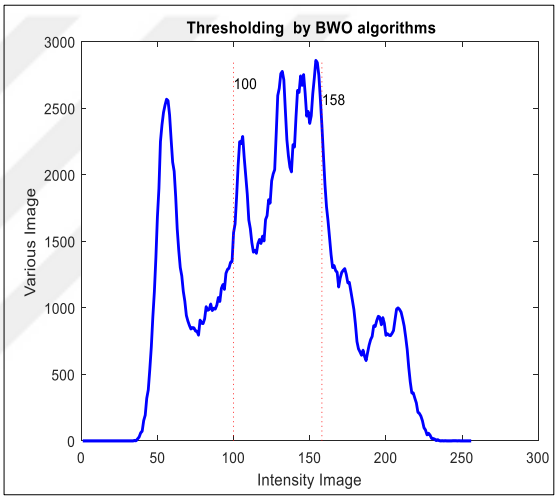

BWO thresholds: 100 and 158

Otsu, m=3

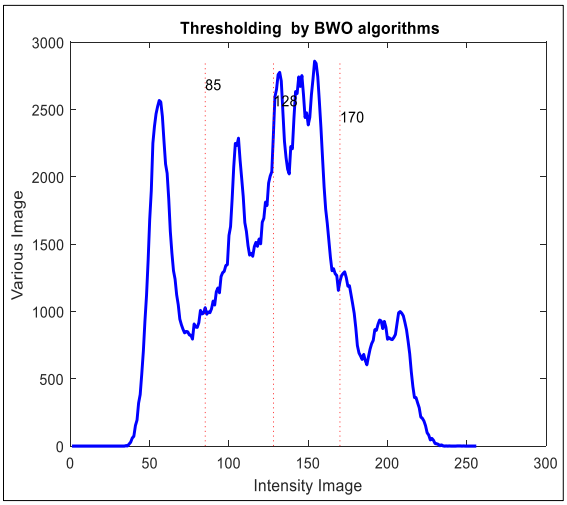

BWO thresholds:85,128,170

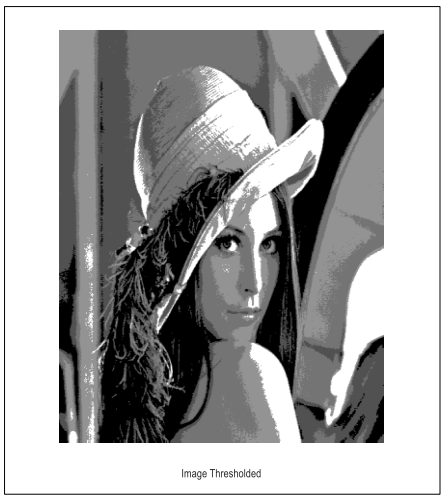

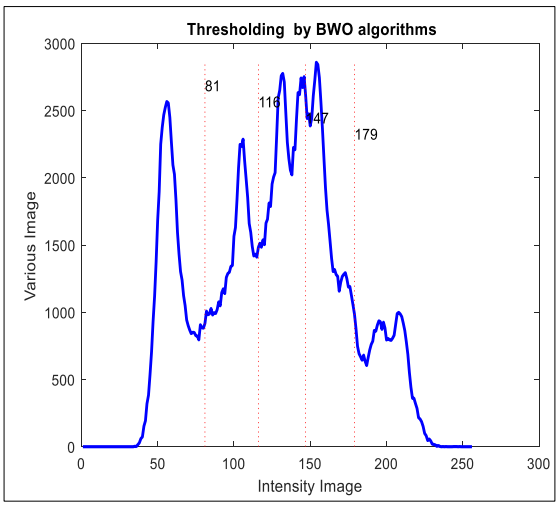

Otsu, m=4 **BWO thresholds:81,116,147,179**

Figure 5.6: Implement the Proposed Method on the Lena Image with Threshold Numbers 1, 2, 3 and 4.

The number of thresholds is 1

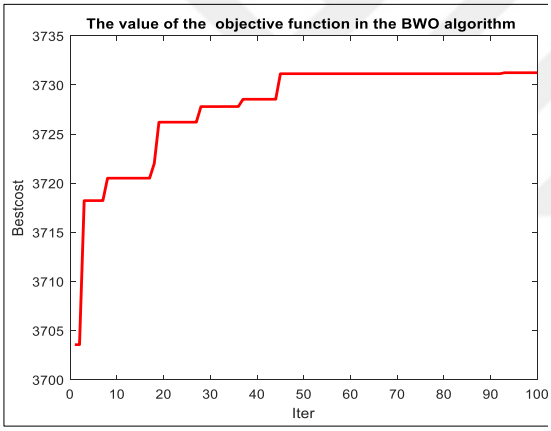

The number of thresholds is 2

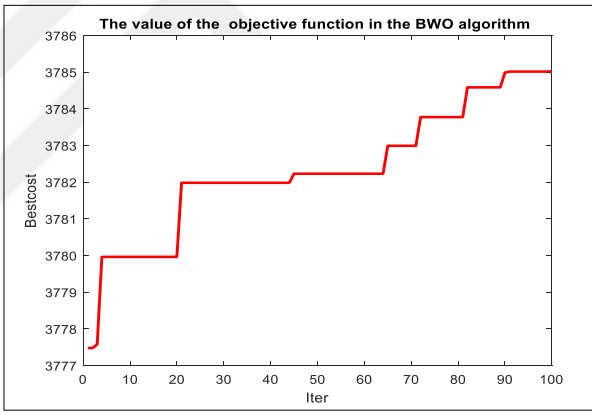

The number of thresholds is 3

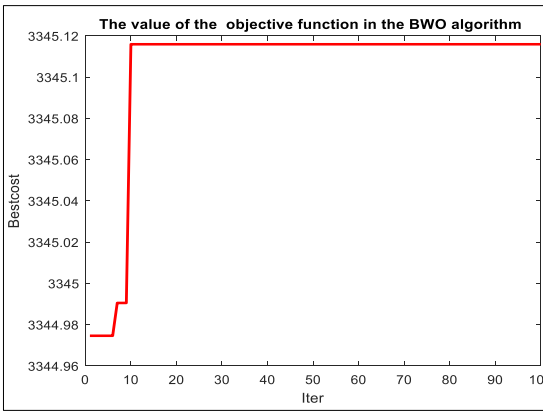

The number of thresholds is 4

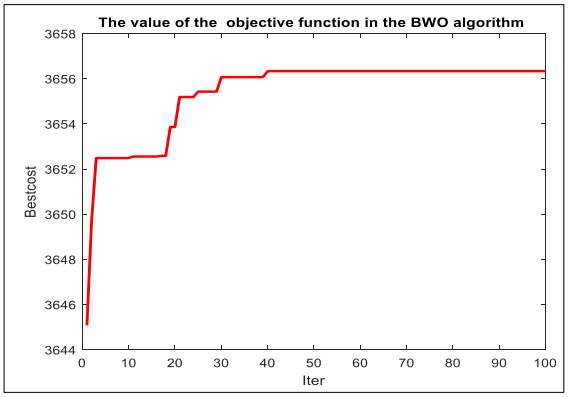

Figure 5.7: The value of the Objective Function in the Cameraman Image in the Proposed Method.

The results of the experiments have demonstrated that the suggested method exhibits optimal outcomes according to the Otsu objective function for both the Cameraman picture at all thresholds the and Peppers photo specifically at 2, 4, and 5 thresholds. Even though most SOS algorithms perform better on Ostrich images, this proposed approach consistently outperforms other competitors by excelling across all three settings applied to Flower and Plane images. In the case of the Girl image when a single threshold is set up, metaheuristic methods including the proposed technique demonstrate similar performance but as soon as it shifts towards two or more than two thresholds, the recommended process proves superior in comparison with other algorithms available. Out of thirty test photos conducted during experimentation, it was noticed that around twenty percent of cases yielded positive outcomes while maximizing the value of Otsu's goal-oriented task via application of the aforementioned method. The algorithm named "black widow" optimization gradually raises the value of the objective function for Otsu thresholding. This method indicates that the proposed approach has determined the most optimal thresholds resulting in values varying slightly from those produced by Otsu thresholding, yet propelling closer to maximizing the target function's value. Tables (5.2) and (5.3) illustrate a comparison between PSNR and SSIM measurements calculated using this methodology with other algorithms such as GA, GWO, ABC, SOS, FA and PSO algorithms.

Table 5.2: The Value of the Objective Function with the Number of Thresholds 1, 2, 3, 4 and 5**.**

	m	BWO	GWO	GA	ABC	SOS	FA	PSO
Cameraman	1	**3346.1452**	3245.1514	3245.1514	3245.1514	3245.1514	3245.1514	3245.1514
	2	**3652.7529**	3609.5601	3609.5470	3609.5601	3609.5601	3609.5601	3609.5601
	3	**3726.3531**	3683.3341	3683.0622	3683.2696	3683.3513	3683.3483	3683.3513
	4	**3786.4412**	3739.2017	3739.0971	3738.6383	3739.2649	3739.2608	3739.2670
	5	**3798.5902**	3769.9434	3769.8053	3768.2473	3770.0157	3770.0536	3770.0570
Peppers	1	2129.3618	2129.3618	2129.3618	2129.3618	2129.3618	2129.3618	2129.3618
	2	**2608.2260**	2532.3214	2532.3156	2532.3214	2532.3214	2532.3214	2532.3214

Table 5.2: The Value of the Objective Function with the Number of Thresholds 1, 2, 3, 4 and 5. "Table Continued"

	3	2698.4105	2703.4915	2703.5436	2703.5364	**2703.5715**	2703.5713	**2703.57**
	4	**2782.0026**	2766.1289	2764.9954	2765.7279	2766.4526	2766.4447	2766.4586
	5	**2832.3314**	2810.2859	2810.1764	2808.7428	2810.8183	2810.8351	2810.8415
Ostrich	1	758.1093	758.1093	758.1093	758.1093	758.1093	758.1093	758.1093
	2	1072.7422	**1074.0847**	1074.0825	**1074.0847**	**1074.0847**	**1074.0847**	**1074.08**
	3	1124.4526	1139.6778	1139.6370	1139.6612	**1139.7081**	1139.6988	1139.7067
	4	1156.0284	1178.5497	1178.4752	1178.2177	**1178.5513**	1178.5488	**1178.55**
	5	1201.4107	1203.4609	1203.0531	1202.2677	1203.4767	1203.5025	**1203.50**
Flower	1	**1298.4520**	1285.6988	1285.6988	1285.6988	1285.6988	1285.6988	1285.6988
	2	**1839.8857**	1823.5081	1823.4972	1823.5081	1823.5081	1823.5081	1823.5081
	3	**2007.1536**	1978.3538	1978.3281	1978.3155	1978.3569	1978.3526	1978.3569
	4	2036.1889	2049.3139	2049.0964	2048.8357	**2049.3689**	2049.3583	**2049.36**
	5	2085.6874	2087.4991	2087.1175	2085.5904	2087.5689	2087.6587	**2087.66**
Plane	1	**441.5442**	436.6506	436.6506	436.6506	436.6506	436.6506	436.6506
	2	**572.4566**	**565.8626**	565.8536	**565.8626**	**565.8626**	**565.8626**	**565.862**
	3	**611.4023**	608.7681	608.8104	608.8317	608.8348	608.8348	608.8348
	4	623.4457	627.1926	627.1837	627.0761	**627.2286**	**627.2286**	**627.228**
	5	635.0238	636.8680	636.7630	636.3327	636.9120	636.9313	**636.931**

Table 5.2: The Value of the Objective Function with the Number of Thresholds 1, 2, 3, 4 and 5. "Table Continued"

Girl	1	1624.3823	1624.3823	1624.3823	1624.3823	1624.3823	1624.3823	1624.3823
	2	**2111.6090**	**2111.6090**	2111.6034	**2111.6090**	**2111.6090**	2111.6055	**2111.6090**
	3	**2216.1875**	2216.1751	2216.0897	2216.1428	**2216.1875**	**2216.1875**	**2216.1875**
	4	**2273.0299**	2269.1948	2268.9041	2268.7985	2269.2496	2269.2473	2269.2491
	5	**2304.8774**	2300.0302	2299.8187	2298.8695	2300.1547	2300.1892	2300.1857

Table 5.3: PSNR Value with a Number of Thresholds 1, 2, 3, 4 and 5**.**

	m	BWO	GWO	GA	ABC	SOS	FA	PSO
Cameraman	1	20.3593	20.3593	20.3593	20.3593	20.3593	20.3593	20.3593
	2	**24.5236**	24.4332	24.4330	24.4332	24.4332	24.4332	24.4332
	3	**26.0854**	26.0787	26.0729	26.0787	26.0788	26.0791	26.0788
	4	**27.9854**	27.9397	27.9372	27.9206	27.9434	27.9425	27.9434
	5	29.4539	29.4534	29.4421	29.3463	29.4539	**29.4578**	29.4573
Peppers	1	19.2449	19.2449	19.2449	19.2449	19.2449	19.2449	19.2449
	2	**22.4486**	22.4392	22.4388	22.4392	22.4392	22.4392	22.4392
	3	25.1272	25.1259	25.1264	25.1270	25.1272	**25.1273**	25.1272
	4	**26.7889**	26.7616	26.7205	26.7504	26.7720	26.7714	26.7721
	5	**28.4886**	28.4518	28.4425	28.3766	28.4774	28.4782	28.4785
Ostrich	1	21.0812	21.0812	21.0812	21.0812	21.0812	21.0812	21.0812
	2	**25.3366**	25.3227	25.3225	25.3227	25.3227	25.3227	25.3227

Table 5.3: PSNR Value with a Number of Thresholds 1, 2, 3, 4 and 5."Table Continued"

	3	27.1408	**27.1500**	27.1475	**27.1500**	27.1478	27.1470	27.1487
	4	28.7593	28.7636	28.7583	28.7475	**28.7640**	28.7638	**28.7640**
	5	30.2489	30.2447	30.2008	30.1608	30.2458	30.2489	**30.2502**
Flower	1	18.6539	18.6539	18.6539	18.6539	18.6539	18.6539	18.6539
	2	**22.7177**	22.7051	22.7053	22.7051	22.7051	22.7051	22.7051
	3	**25.2664**	25.2612	25.2588	25.2588	25.2614	25.2607	25.2614
	4	27.2381	27.2423	27.2297	27.2213	**27.2436**	27.2421	**27.2436**
	5	28.8534	28.8582	28.8280	28.7623	28.8602	**28.8656**	**28.8656**
Plane	1	24.6383	24.6383	24.6383	24.6383	24.6383	24.6383	24.6383
	2	**28.3856**	28.3823	28.3811	28.3823	28.3823	28.3823	28.3823
	3	**31.0446**	31.0119	31.0205	31.0179	31.0204	31.0204	31.0204
	4	**32.9787**	32.9420	32.9395	32.9301	32.9523	32.9523	32.9525
	5	**34.4884**	34.4449	34.4398	34.3520	34.4453	34.4467	34.4458
Girl	1	19.3745	19.3640	19.3640	19.3640	19.3640	19.3640	19.3640
	2	**23.9024**	23.8906	23.8904	23.8906	23.8906	23.8905	23.8906
	3	**26.0896**	26.0670	26.0658	26.0659	26.0674	26.0674	26.0674
	4	27.7899	27.8039	27.7978	27.7898	27.8053	**27.8068**	27.8063
	5	**29.2906**	29.2727	29.2621	29.2023	29.2798	29.2822	29.2822

Table 5.4: SSIM Value with a Number of Thresholds 1, 2, 3, 4 and 5**.**

	m	BWO	GWO	GA	ABC	SOS	FA	PSO
Cameraman	1	0.7404	0.7404	0.7404	0.7404	0.7404	0.7404	0.7404
	2	**0.7866**	0.7845	0.7846	0.7845	0.7845	0.7845	0.7845
	3	**0.8286**	0.8273	0.8264	0.8278	0.8275	0.8276	0.8275
	4	**0.8375**	0.8350	0.8349	0.8337	0.8352	0.8352	0.8352
	5	0.8649	0.8642	**0.8643**	0.8629	0.8639	0.8642	0.8641
Peppers	1	0.6273	0.6273	0.6273	0.6273	0.6273	0.6273	0.6273
	2	**0.6729**	0.6728	0.6727	0.6728	0.6728	0.6728	0.6728
	3	**0.7062**	0.7056	0.7054	0.7055	0.7053	0.7053	0.7053
	4	0.7319	0.7316	0.7299	0.7313	**0.7323**	0.7321	**0.7323**
	5	**0.7658**	0.7649	0.7642	0.7647	0.7651	0.7651	0.7651
Ostrich	1	0.7894	0.7894	0.7894	0.7894	0.7894	0.7894	0.7894
	2	**0.8461**	**0.8461**	0.8460	**0.8461**	**0.8461**	**0.8461**	**0.8461**
	3	**0.8594**	**0.8594**	0.8592	0.8592	0.8593	0.8592	0.8593
	4	**0.8781**	0.8771	0.8772	0.8772	0.8771	0.8771	0.8771
	5	**0.8924**	0.8898	0.8911	0.8885	0.8898	0.8901	0.8899
Flower	1	0.5153	0.5153	0.5153	0.5153	0.5153	0.5153	0.5153
	2	0.7159	0.7159	0.7159	0.7159	0.7159	0.7159	0.7159

Table 5.4: SSIM Value with a Number of Thresholds 1, 2, 3, 4 and 5."Table Continued"

	3	0.7886	0.7889	0.7887	**0.7891**	0.7888	0.7888	0.7888
	4	0.8390	0.8392	**0.8398**	0.8396	0.8393	0.8393	0.8393
	5	**0.8728**	0.8718	0.8702	0.8696	0.8720	0.8720	0.8720
Plane	1	0.9192	0.9192	0.9192	0.9192	0.9192	0.9192	0.9192
	2	**0.9017**	0.9017	0.9015	**0.9017**	**0.9017**	**0.9017**	**0.9017**
	3	**0.9041**	0.9037	0.9037	0.9039	**0.9041**	**0.9041**	**0.9041**
	4	**0.9013**	0.9000	0.9003	0.9009	0.8994	0.8994	0.8994
	5	**0.9161**	0.9157	0.9153	0.9141	0.9157	**0.9161**	**0.9161**
Girl	1	0.4455	0.4455	0.4455	0.4455	0.4455	0.4455	0.4455
	2	0.6469	0.6469	0.6469	0.6469	0.6469	0.6469	0.6469
	3	0.7622	0.7619	**0.7623**	0.7621	0.7620	0.7620	0.7620
	4	**0.8211**	0.8206	0.8202	0.8202	0.8202	0.8205	0.8204
	5	**0.8571**	0.8562	0.8565	0.8559	0.8564	0.8567	0.8567

The superiority of a threshold algorithm can be seen in its PSNR and SSIM maximum values. The relevant tables provide experimental results showing that the proposed method yields better objective function, PSNR, and SSIM values than competing methods. The aggregate of these three metrics indicates that the proposed approach achieves a superior threshold on the photos. Based on the results of the aforementioned trials, Tables (5.3) and (5.4) reveal that the proposed strategy typically yields better PSNR and SSIM values. The results show that the suggested method outperforms the alternatives as the number of thresholds grows. When using a single or double threshold, the proposed method yields the same results as

competing methods. Increases in threshold number and complexity make the suggested technique superior to other meta-algorithms of a similar kind since it yields more PSNR and SSIM indicators. The results of 30 trials reveal that, on average, 25 of the offered solutions get a higher PSNR index, which is equivalent to about 83.33 percent of all experiments. The proposed technique offers support for around eighty percent of the total number of experiments included in the SSIM index. In terms of the PSNR and SSIM indices, the proposed method achieves results that are superior to those obtained by the gray wolf optimization algorithm, the genetic algorithm, the artificial bee colony algorithm, the symbiotic organisms search algorithm, the firefly algorithm, and the particle swarm optimization algorithm in 83.33 and 80 percent of the cases, respectively.

5.4.2 Runtime

One of the most crucial metrics for judging the effectiveness of the suggested algorithm and other meta-heuristic algorithms is the runtime of thresholding techniques. In this case, 50 iterations are performed on the Intel 5-core processor with 6 GB of RAM using a population size of 20, and 100 repetitions are performed. Execution time analysis findings are shown in Figure (5.8) for all of these methods. You can see how each proposed algorithm and metaheuristic compares to the Atsu threshold in terms of execution time in the table below. Otsu's thresholding execution time as a percentage of the speedup provided by metaheuristic algorithms is also displayed in Figure (5.9).

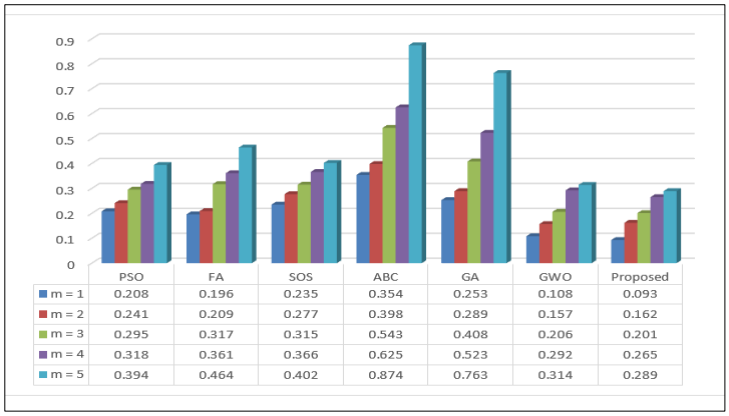

	PSO	FA	SOS	ABC	GA	GWO	Proposed
m = 1	0.208	0.196	0.235	0.354	0.253	0.108	0.093
m = 2	0.241	0.209	0.277	0.398	0.289	0.157	0.162
m = 3	0.295	0.317	0.315	0.543	0.408	0.206	0.201
m = 4	0.318	0.361	0.366	0.625	0.523	0.292	0.265
m = 5	0.394	0.464	0.402	0.874	0.763	0.314	0.289

Figure 5.8: Comparison of the Average Execution Time in the Proposed Method with Other Algorithms.

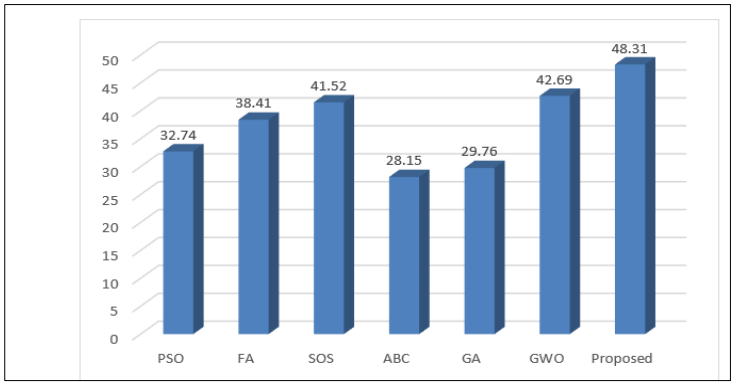

Figure 5.9: Comparison of Execution Speedup in the Proposed Method with Other Algorithms.

The experimental results for both the metaheuristic and suggested algorithms show that their execution time scales linearly with the threshold number from 1 to 5. Otsu's execution time increases from 1.36 seconds to 145.87, or about 107.25 times, from 1 to 5 in some studies, although the execution time of the suggested algorithm and other alternatives both climb by a small amount as the number of thresholds is increased. This suggests that the Otsu algorithm's performance has degraded significantly as the number of thresholds has grown, and that it lacks the efficiency required for multi-level thresholds, in comparison to alternative meta-heuristic approaches, which take significantly less time. When compared to the average speedup rate over all thresholds for the other meta-heuristic algorithms, the acceleration values for the proposed approach, GWO, GA, ABC, SOS, FA, and PSO are 48.31, 42.69, 28.76, 28.15, 41.52, 38.41, and 32.74, respectively.

5.4.3 Sustainability

The standard deviation (SD) test is a useful metric for judging the quality of threshold algorithms like the one provided here and other meta-algorithms. Several approaches, including the one described here, are given in Table (5.5) for calculating the objective function, a crucial metric in the Otsu threshold algorithm. Experiments indicate that the suggested method is more stable than existing meta-heuristic algorithms due to its smaller standard deviation in most materials. Therefore, the proposed method can be used to achieve the best possible standard deviation in the Otsu thresholding goal function.

Table 5.5: Standard Deviation Index in Standard Images with A number of Thresholds 1, 2, 3, 4 and 5.

	m	BWO	GWO	GA	ABC	SOS	FA	PSO
Cameraman	1	0.0	0.0	0.0	0.0	0.0	0.0	0.0
	2	0.0	0.0	0.0	0.0	0.0	0.0	0.0
	3	0.0	0.06780	0.42091	0.06579	0.0	0.0	0.0
	4	0.0	0.25043	0.33855	0.38047	0.0	0.02005	0.0
	5	0.00847	0.25406	0.29073	0.91146	0.13524	0.01120	0.00931
Peppers	1	0.0	0.0	0.0	0.0	0.0	0.0	0.0
	2	0.0	0.0	0.06833	0.0	0.0	0.0	0.0
	3	0.0	0.06697	0.06845	0.18141	0.0	0.0	0.0
	4	0.04454	0.14994	1.68477	0.54054	0.04454	0.02177	0.0
	5	0.0	0.28493	0.32652	1.01875	0.10717	0.0	0.0
Ostrich	1	0.0	0.0	0.0	0.0	0.0	0.0	0.0
	2	0.0	0.0	0.01008	0.0	0.0	0.0	0.0
	3	0.0	0.02802	0.08687	0.04030	0.0	0.01204	0.00246
	4	0.00064	0.00394	0.41428	0.26530	0.00080	0.02031	0.00110
	5	0.05862	0.23505	0.45084	0.73895	0.12565	0.02583	0.00010
Flower	1	0.0	0.0	0.0	0.0	0.0	0.0	0.0
	2	0.0	0.0	0.01693	0.0	0.0	0.0	0.0
	3	0.0	0.00951	0.09407	0.09901	0.0	0.00808	0.0
	4	0.00645	0.29076	0.23248	0.44650	0.00707	0.01682	0.0
	5	0.00107	0.46337	0.73223	0.88794	0.12788	0.02529	0.00121
Plane	1	0.0	0.0	0.0	0.0	0.0	0.0	0.0
	2	0.0	0.0	0.00812	0.0	0.0	0.0	0.0
	3	0.0	0.21552	0.04477	0.04033	0.0	0.0	0.0
	4	0.0	0.09625	0.09581	0.12811	0.0	0.00150	0.0
	5	0.00075	0.0	0.0	0.0	0.0	0.0	0.0
Girl	1	0.0	0.0	0.0	0.0	0.0	0.0	0.0
	2	0.0	0.06780	0.42091	0.06579	0.0	0.0	0.0
	3	0.0	0.25043	0.33855	0.38047	0.0	0.02005	0.0
	4	0.00854	0.25406	0.29073	0.91146	0.13524	0.01120	0.00931

5.4.5 Application in Medical Imaging

The segmentation of medical images is a crucial use case for threshold algorithms like Otsu. With the proposed method and Otsu thresholding techniques, medical picture analysis is feasible. Extraction of brain tumours in magnetic resonance imaging of the brain is one of the key uses of proposed thresholds, as illustrated in Figure (5.10).

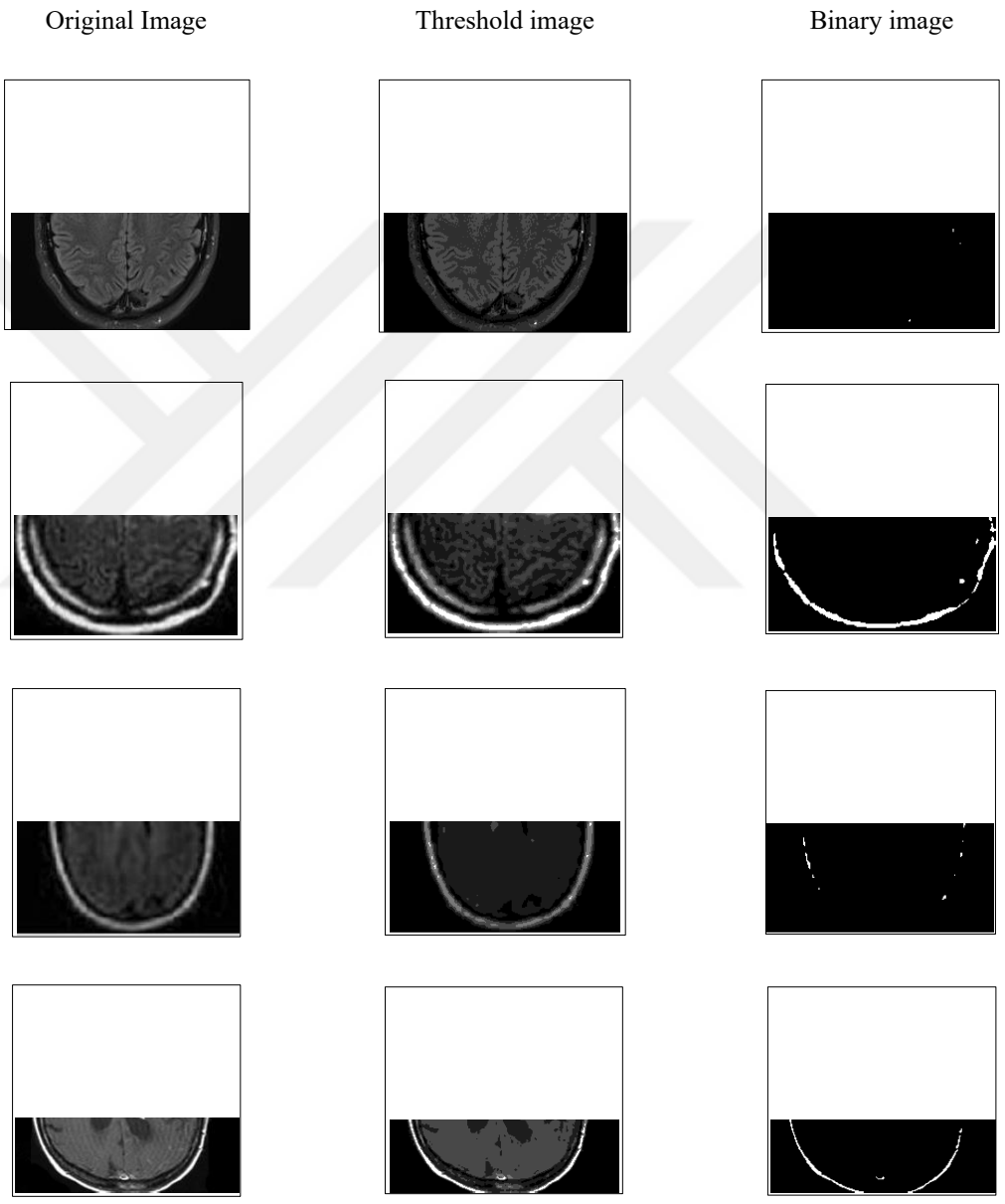

Figure 5.10: Application of the Proposed Algorithm in the Segmentation Brain Tumors.

The researchers utilized an MRI scan of the patient's brain tumor as a specimen in their investigations. During the experimentation, they scrutinized the images and endeavored to pinpoint with precision the location of tumors within subjects' brains that were under scrutiny. The left-hand side picture is a magnetic resonance imaging scan illustration of the said tumor while on right-hand side depict microscopic photograph evidence from identical regions. An elaborate representation delineating Otsu technique feature prominently n mid-image whereas binary image has been shown towards its right where instances of singular white dots serve as manifestations for tumors visible in brain scans obtained via this method. Overall findings state convincingly that algorithm proposed by researchers was successful since it managed to identify multi-levels demonstrated by MRI scans when imparted with starting threshold values equaling 4,7,6 and4 corresponding each time respectively amongst first four samples surveyed during research procedures. Upon generating the tumor, it is subsequently emphasized at the center of the image through binarization applied to the earlier selected image. The identification of optical lenses on retinal images is a vital application that can gain advantages from multi-level thresholding approaches suggested in this paper. Experimental illustrations verifying the efficacy of this technique for identifying these locations in photographs of retina are illustrated in figure (5.11).

Original Image Threshold image Binary image

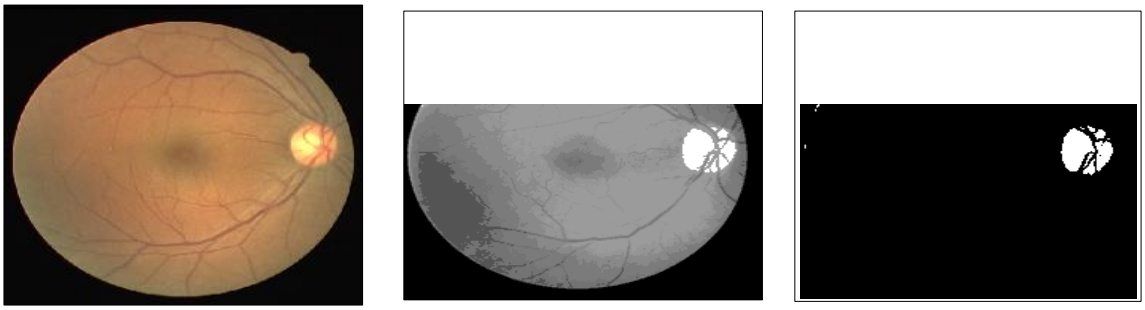

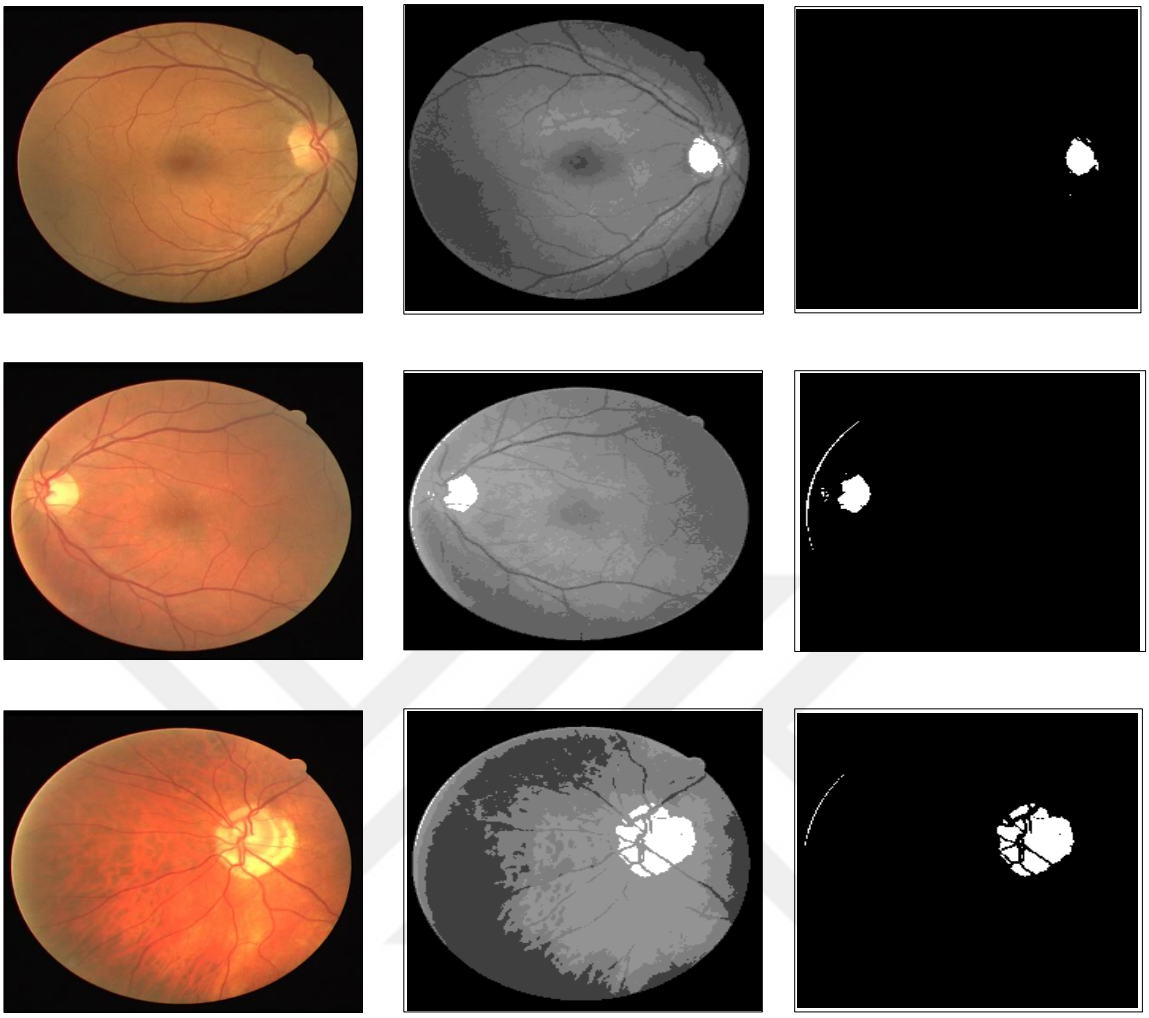

Figure 5.11: Application of The Proposed Algorithm in Segmentation the Optic Image.

There is a color image of the eye on the left, a binary image on the right, and a threshold image calculated using the provided approach. It is clear that the suggested method is able to determine, to a significant extent, the parts of the image that correspond to the lena of the eye accurately.

5.5 Encrpytion Pahse Results

The results presented in the Table (5.6) and Figure (5.12) shows the performance measurements of various techniques and algorithms for accomplishing a specific task, which comprises Peak Signal-to-Noise Ratio, Unified Average Changing Intensity and Encryption Quality. Diverse approaches report different values for each indicator.

Table 5.6: Various Performance Metrics.

Reference		PSNR	UACI	Encryption Quality
Narasimhan and Arunachalam, 2019 [38]		20.3593	5.5096	7.9197
Kiran et al., (2020) [45]	Baby	40.5949	12.3073	3.2067
	Baby Womb	32.6951	32.0196	6.8615
	MRI	32.6951	15.5345	4.7368
	Hand	30.5238	11.7870	4.3455
	Foot	32.3488	8.1099	3.8080
Shalaby et al., (2020)[46]		∞	31.438%	98
Romero-Arellano et al., (2021) [59]		29.4539	33.4469	79.9998
Proposed		29.4539	33.02%	100

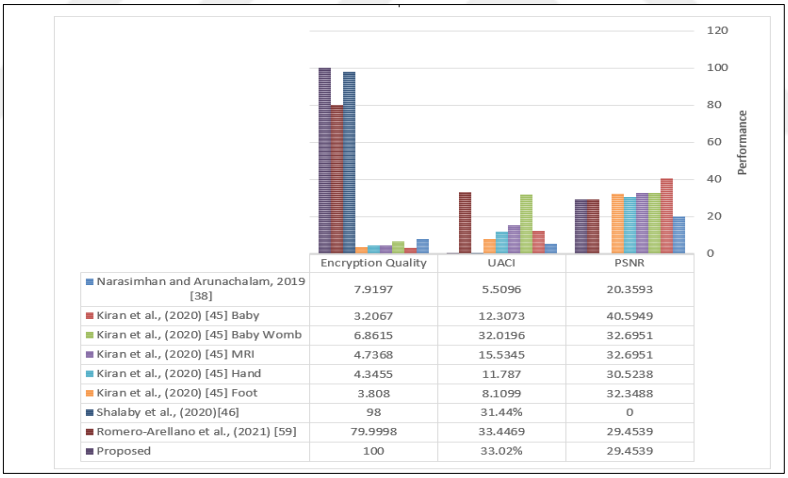

Figure 5.12: Algorithms Performance Evaluation .

As per Narasimhan and Arunachalam's 2019 investigation, their proposed method yielded an PSNR equalling to 20.3593, UACI equalling to 5.5096 while attaining the encryption quality score of 7.9197; indicating substantial non-controversial pixel ratio, moderate peak signal -to-noise ratio with comparatively low unified average changing intensity as well as moderate encryption quality or strength value respectively. Kiran et al. conducted an experiment employing different image types, such as Baby, Baby Womb, MRI, Hand and

Foot. The outcomes revealed that for images of babies the proposed method produced PSNR at 40.5949%, UACI at 12.3073% and Encryption Quality value of 3.2067%. Comparable results were obtained for other pictures studied in this research work which showed moderate performance concerning PSNR but yielded lesser Encryption Quality values while exhibiting higher UACI figures than expected previously.

In another study by Shalaby et al., a high non-controversial pixel ratio was achieved with PSNR or UACI thereby making it indecipherable how well the model performed regarding those metrics mentioned above; although yielding highly satisfactory results in terms of maintaining non-controversial pixels present within the image tested in their system-reflecting precise outputs on fewer known evaluation criteria metrics from previous studies mentioned earlier in comparison with them where detailed measurements have been done on almost every aspect related to its output attainment level accuracy rate calculation methodology applied under certain specified conditions analysis framework used systematically like. According to Romero-Arellano et al., the method presented in this research attained a peak signal-to-noise ratio of 29.4539, an average unified changing intensity of 33.4469 and high encryption quality with a score of 79.9998 based on its evaluation metrics analysis results. These outcomes indicate that the model achieved impressive performance for non-controversial pixels without subjective interpretation, moderate noise reduction capability, significant changes preservation ability while maintaining excellent level data protection due to reliable encryption quality output given acceptable values from statistics heuristics measures.

The method proposed in this study achieved a peak signal-to-noise ratio of 29.4539, a unified average changing intensity of 33.02% and an excellent encryption quality score. Various studies have demonstrated different outcomes regarding the effectiveness metrics for this task; nonetheless, our research has shown promising results with high values concerning PSNR, UACI, as well as Encryption Quality measures. When a thresholding strategy is used, the accuracy of the algorithm may be evaluated based on which values of SSIM are the highest. This evaluation can be performed both before and after applying the strategy. The strategy that was suggested was successful in obtaining values for the objective function, PSNR, and SSIM the majority of the time, despite the outcomes of the trials that were contained in the tables that were queried. This was the case regardless of the fact that the tables were queried. In point of fact, that the proposed method has the maximum possible

sum of these three signs lends credence to the notion that it offers a noticeably larger threshold for the number of photos. In Table (5.7), the influence that each of these parameters has on the encryption and decryption procedures is broken down in detail.

Table 5.7: Encryption Quality Measurements.

Data	Threshold	SSIM
	3346.1452	0.9673
	2129.3618	0.9729
	758.1093	0.9862
	1298.4520	0.9919
	1624.3823	0.9658

Figure (5.13) and (5.14) presents an analysis of various data samples by using the Structural Similarity Index Measure at different thresholds. SSIM is a commonly used parameter for measuring similarity between two sets of images or, in this context, two datasets. The larger the value of SSIM, the more alike those sets are perceived to be. Accordingly, among all tested scenarios in this research project at varying thresholds utilizing SSIM as a metric for evaluation purposes; higher similarities were found when comparing sample data with one another closely at 1298.4520 threshold leading up to maximum observed SSIM score (0.9919). This result provides an indication that these particular dataset features exhibit strong correlation and resemblance among themselves compared to other examined ones where lower levels of correlation have been detected under similar conditions - such as observation range around 1624.3823 establishing a minimum observed SSI value about 0.9658 - on comparison with corresponding benchmarks during analysis done throughout said investigation process.

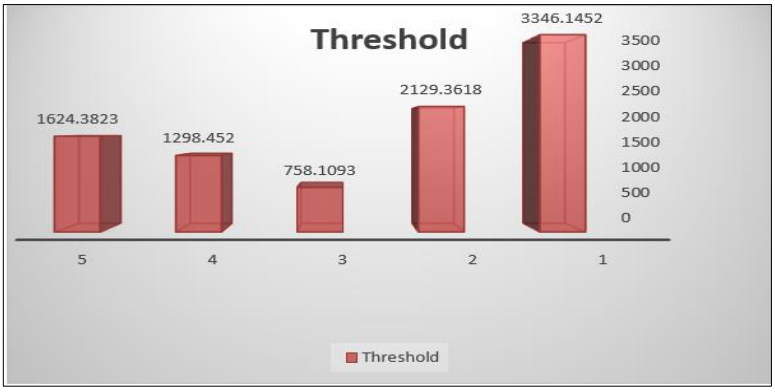

Figure 5.13: Threshold Performance Evaluation .

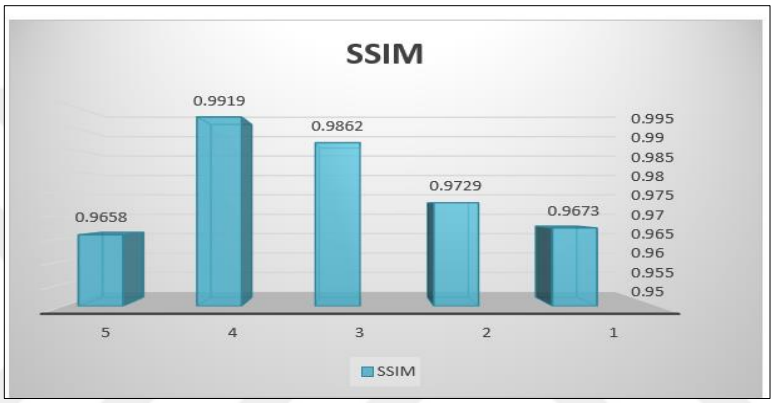

Figure 5.14: SSIM Performance Evaluation.

When considering two samples as similar, a higher threshold means that a stricter criterion is used. The research findings indicate that using lower thresholds (such as 758.1093 and 1298.4520) lead to higher values for Structural Similarity Index Measure, which denotes a greater degree of similarity between the compared data samples. Conversely, utilizing higher thresholds (like 1624.3823) leads to lower SSIM values indicating decreased similarity. The results show that there is a clear correlation between high UACI values and a noticeable change in pixel values between the original image and the encrypted image, which is indicative of the encryption's efficacy and, by extension, the difficulty with which attackers can obtain sensitive information.

6. DISCUSSION AND CONCLUSIONS

Image processing applications, such as diagnosing brain tumours, rely heavily on being able to locate and pinpoint the location of an object's edges and boundaries. Using thresholds in images is a crucial technique for detecting edges and segmenting images. The histogram is used to establish a series of thresholds that categorize the image into different groups according on the amount of light present. Generally speaking, thresholds are used for segmentation and to reduce the number of light intensity levels in an image. In addition to their use in analysing traffic and agricultural data, thresholds have also been put to use in the study of medical imaging. Many picture thresholding techniques, including those based on image histograms, seek to determine the optimal luminance level at which an image may be properly categorized. Histograms from the Otsu technique form the basis of one of the threshold approaches. The increasing complexity of the procedure in Otsu thresholding as the number of thresholds increases is a major drawback that renders the method impractical in many settings. In order to address concerns regarding execution time, this research makes an effort to improve the threshold in Otsu by utilizing a swarm intelligence algorithm. More specifically, the black widow optimization technique is being utilized. The proposed method is ANALYSED and assessed in comparison to GWO, ABC, SOS, FA, and PSO in terms of the mean Otsu objective function, PSNR, and SSIM, as well as the minimal execution time and standard deviation. Experiments have demonstrated that the performance of various metaheuristic algorithms is roughly equivalent when only one or two criteria are taken into consideration. The suggested method produces a higher value for the objective function, as well as larger values for the PSNR and SSIM index, and it runs faster than the existing meta-heuristic algorithms. Increasing the total number of thresholds utilized in the procedure brings about this desired result. Experimentation has demonstrated that the proposed standard deviation is very small and very close to zero, which suggests that the method is more stable than other methods that are currently available. The method that was suggested has a useful use in the separation of visual images and MRI scans of the brain. The effectiveness of the proposed procedure in removing malignant or optically aberrant regions of the eye has been shown through experiments carried out using medical sample photographs. This line of inquiry aims to present such a strategy as one of its goals, and the

method that has been proposed will also be employed as a thresholding technique in future studies to suggest the binarization of areas in medical imaging.

Since raising the number of thresholds in the approach raises the value of the target function, and the pre-processing method described enhances the PSNR and SSIM indices, the suggested method is more accurate than earlier meta-heuristic methods and takes less time to run. In this thesis, the developed method is put to use segmenting iris images. The eyes' iris regions can be extracted successfully in experiments utilizing medical sample photographs. The iris template stored in the database is encrypted using AES techniques in the proposed system. Images stored in the database are protected from unauthorized access by being encrypted before being used in critical security applications. The images stored in the database are encrypted, so only those with the private key can view the originals.

This research may be taken in a few different directions in the future. To begin, it would be advantageous to optimize the implementation so that the benefits of a multilevel method could be realized. In terms of the amount of work that needs to be done on the computation, as well as the amount of storage space required, multilevel methods can achieve linear complexity. Another approach could be to refine the measurements using additional optimization algorithms. This would be an alternative course of action. in addition to the possibility of integrating two or more algorithms to further enhance the system's already impressive level of security.

REFERENCES

[1] V. Wiley and T. Lucas, “Computer Vision and Image Processing: A Paper Review,” International Journal of Artificial Intelligence Research, vol. 2, no. 1, 2018.

[2] Kotappa Y G, Krushika M, M Ravichandra, and Mrs. Pranitha, “A Review Paper on Computer Vision and Image Processing,” International Journal of Advanced Research in Science, Communication and Technology, 2022.

[3] A. Gupta, “Current research opportunities for image processing and computer vision,” Computer Science, vol. 20, no. 4, 2019.

[4] C. Kang, C. Wu, and J. Fan, “Lorenz curve-based entropy thresholding on circular histogram,” IEEE Access, vol. 8, 2020.

[5] U. K. Malviya, “Tumor Detection in MRI Images using Modified Multi-level Otsu Thresholding (MLOT) and Cross-Correlation of Principle Components,” in Proceedings of the 4th International Conference on Computing Methodologies and Communication, ICCMC 2020, 2020.

[6] B. Vinoth Kumar, S. Sabareeswaran, and G. Madumitha, “A Decennary Survey on Artificial Intelligence Methods for Image Segmentation,” in Advances in Intelligent Systems and Computing, 2020.

[7] C. Bhuvan, S. Bansal, R. Gupta, and A. Bhan, “Computer based diagnosis of malaria in thin blood smears using thresholding-based approach,” in 2020 7th International Conference on Signal Processing and Integrated Networks, SPIN 2020, 2020

[8] N. D. Hoang, “Image Processing-Based Pitting Corrosion Detection Using Metaheuristic Optimized Multilevel Image Thresholding and Machine-Learning Approaches,” Math Probl Eng, vol. 2020, 2020.

[9] R. S. Gargees and G. J. Scott, “Large-scale, multiple level-of-detail change detection from remote sensing imagery using deep visual feature clustering,” Remote Sens (Basel), vol. 13, no. 9, 2021.

[10] T. Y. Goh, S. N. Basah, H. Yazid, M. J. Aziz Safar, and F. S. Ahmad Saad, “Performance analysis of image thresholding: Otsu technique,” Measurement (Lond), vol. 114, 2018.

[11] A. T. H. Al-Rahlawee and J. Rahebi, “Multilevel thresholding of images with improved Otsu thresholding by black widow optimization algorithm,” Multimed Tools Appl, vol. 80, no. 18, 2021.

[12] B. Küçükuğurlu and E. Gedikli, “Symbiotic Organisms Search Algorithm for multilevel thresholding of images,” Expert Syst Appl, vol. 147, 2020.

[13] M. A. Elaziz, A. A. Ewees, and D. Oliva, “Hyper-heuristic method for multilevel thresholding image segmentation,” Expert Syst Appl, vol. 146, 2020.

[14] S. J. Mousavirad and H. Ebrahimpour-Komleh, “Human mental search-based multilevel thresholding for image segmentation,” Appl Soft Comput, vol. 97, 2020.

[15] M. H. Merzban and M. Elbayoumi, “Efficient solution of Otsu multilevel image thresholding: A comparative study,” Expert Syst Appl, vol. 116, 2019.

[16] A. Hemeida, R. Mansour, and M. E. Hussein, “Multilevel Thresholding for Image Segmentation Using an Improved Electromagnetism Optimization Algorithm,” International Journal of Interactive Multimedia and Artificial Intelligence, vol. 5, no. 4, 2019.

[17] D. Oliva, S. Hinojosa, E. Cuevas, G. Pajares, O. Avalos, and J. Gálvez, “Cross entropy-based thresholding for magnetic resonance brain images using Crow Search Algorithm,” Expert Syst Appl, vol. 79, 2017.

[18] H. Ramadan, C. Lachqar, and H. Tairi, “A survey of recent interactive image segmentation methods,” Computational Visual Media, vol. 6, no. 4. 2020.

[19] Z. Niu and H. Li, “Research and analysis of threshold segmentation algorithms in image processing,” in Journal of Physics: Conference Series, 2019.

[20] A. K. Bhandari, N. Singh, and I. V. Kumar, “Lightning search algorithm-based contextually fused multilevel image segmentation,” Applied Soft Computing Journal, vol. 91, 2020.

[21] R. Girshick, J. Donahue, T. Darrell, and J. Malik, “Region-Based Convolutional Networks for Accurate Object Detection and Segmentation,” IEEE Trans Pattern Anal Mach Intell, vol. 38, no. 1, pp. 142–158, Jan. 2016.

[22] Y. Zhan and G. Zhang, “An improved OTSU algorithm using histogram accumulation moment for ore segmentation,” Symmetry (Basel), vol. 11, no. 3, 2019.

[23] L. He and S. Huang, “An efficient krill herd algorithm for color image multilevel thresholding segmentation problem,” Applied Soft Computing Journal, vol. 89, 2020.

[24] W. Liu, H. Shi, S. Pan, Y. Huang, and Y. Wang, “An Improved Otsu Multi-Threshold Image Segmentation Algorithm Based on Pigeon-Inspired Optimization,” in Proceedings - 2018 11th International Congress on Image and Signal Processing, BioMedical Engineering and Informatics, CISP-BMEI 2018, 2019.

[25] X. Xia, H. Gao, H. Hu, R. Lan, and C. M. Pun, “A Multi-Level Thresholding Image Segmentation Based on an Improved Artificial Bee Colony Algorithm,” in EAI/Springer Innovations in Communication and Computing, 2020.

[26] L. Xiao, H. Ouyang, and C. Fan, “An improved Otsu method for threshold segmentation based on set mapping and trapezoid region intercept histogram,” Optik (Stuttg), vol. 196, 2019.

[27] M. Benssalah, Y. Rhaskali, and M. S. Azzaz, “Medical Images Encryption Based on Elliptic Curve Cryptography and Chaos Theory,” in 2018 International Conference on Smart Communications in Network Technologies, SaCoNeT 2018, 2018.

[28] N. S. Rani, U. Karthik, and S. Ranjith, “Extraction of Gliomas from 3D MRI Images using Convolution Kernel Processing and Adaptive Thresholding,” in Procedia Computer Science, 2020.

[29] A. K. M. Khairuzzaman and S. Chaudhury, “Brain MR image multilevel thresholding by using particle swarm optimization, otsu method and anisotropic diffusion,” International Journal of Applied Metaheuristic Computing, vol. 10, no. 3, 2019.

[30] P. Y. Yin and T. H. Wu, “Multi-objective and multi-level image thresholding based on dominance and diversity criteria,” Applied Soft Computing Journal, vol. 54, 2017.

[31] I. H. Latif, “Time Evaluation of Different Cryptography Algorithms Using Labview,” in IOP Conference Series: Materials Science and Engineering, 2020.

[32] O. G. Abood, M. A. Elsadd, and S. K. Guirguis, “Investigation of cryptography algorithms used for security and privacy protection in smart grid,” in 2017 19th International Middle-East Power Systems Conference, MEPCON 2017 - Proceedings, 2018.

[33] Ratnadewi, R. P. Adhie, Y. Hutama, A. Saleh Ahmar, and M. I. Setiawan, “Implementation Cryptography Data Encryption Standard (DES) and Triple Data Encryption Standard (3DES) Method in Communication System Based Near Field Communication (NFC),” in Journal of Physics: Conference Series, 2018.

[34] M. Khaled Elbeltagy, “StegoCrypt3D: 3D Object and Blowfish”.

[35] B. Verma and S. Malhotra, “SECURE IMAGE PROCESSING USING AES ALGORITHM.”

[36] A. Arab, M. J. Rostami, and B. Ghavami, “An image encryption method based on chaos system and AES algorithm,” Journal of Supercomputing, vol. 75, no. 10, pp. 6663–6682, 2019.

[37] Y. E. Ö. and J. R. A. S. Abdullah, “A novel method for retinal optic disc detection using bat meta-heuristic algorithm,” *Medical & Biological Engineering & Computing*, vol. 56, no. 11, pp. 2015–2024, 2018.

[38] S. Narasimhan and M. Arunachalam, “Bio-PUF-MAC authenticated encryption for iris biometrics,” Comput Intell, vol. 36, no. 3, pp. 1221–1241, 2020.

[39] S. Pathan, P. Kumar, R. Pai, and S. v. Bhandary, “Automated detection of optic disc contours in fundus images using decision tree classifier,” Biocybern Biomed Eng, vol. 40, no. 1, pp. 52–64, 2020.

[40] Y. Liu, J. Sun, H. Yu, Y. Wang, and X. Zhou, “An improved grey wolf optimizer based on differential evolution and OTSU algorithm,” Applied Sciences (Switzerland), vol. 10, no. 18, 2020.

[41] D. J. Derwin, S. T. Selvi, and O. J. Singh, “Secondary Observer System for Detection of Microaneurysms in Fundus Images Using Texture Descriptors,” J Digit Imaging, vol. 33, no. 1, pp. 159–167, 2020.

[42] S. Wang, H. Jia, and X. Peng, “Modified salp swarm algorithm based multilevel thresholding for color image segmentation,” Mathematical Biosciences and Engineering, vol. 17, no. 1, pp. 700–724, 2020.

[43] J. R. H. Kumar, C. S. Seelamantula, Y. S. Kamath, and R. Jampala, “Rim-to-Disc Ratio Outperforms Cup-to-Disc Ratio for Glaucoma Prescreening,” Sci Rep, vol. 9, no. 1, 2019.

[44] J. Mao *et al.*, “Automated diagnosis and quantitative analysis of plus disease in retinopathy of prematurity based on deep convolutional neural networks,” Acta Ophthalmol, vol. 98, no. 3, pp. e339–e345, 2020.

[45] Kiran, B. D. Parameshachari, H. T. Panduranga, and S. L. Ullo, “Analysis and Computation of Encryption Technique to Enhance Security of Medical Images,” in IOP Conference Series: Materials Science and Engineering, IOP Publishing Ltd, 2020.

[46] M. A. W. Shalaby, M. T. Saleh, and H. N. Elmahdy, “Enhanced Arnold’s Cat Map-AES Encryption Technique for Medical Images,” in *2nd Novel Intelligent and Leading Emerging Sciences Conference, NILES 2020*, Institute of Electrical and Electronics Engineers Inc., pp. 288–295,2020.

[47] D. Devarajan, S. M. Ramesh, and B. Gomathy, “A metaheuristic segmentation framework for detection of retinal disorders from fundus images using a hybrid ant colony optimization,” Soft comput, vol. 24, no. 17, pp. 13347–13356, 2020.

[48] L. Abdel-Hamid, “Glaucoma Detection from Retinal Images Using Statistical and Textural Wavelet Features,” J Digit Imaging, vol. 33, no. 1, pp. 151–158, Feb. 2020.

[49] R. G. Ramani and J. J. Shanthamalar, “Improved image processing techniques for optic disc segmentation in retinal fundus images,” Biomed Signal Process Control, vol. 58, Apr. 2020.

[50] D. A. Dharmawan, B. P. Ng, and S. Rahardja, “A new optic disc segmentation method using a modified Dolph-Chebyshev matched filter,” Biomed Signal Process Control, vol. 59,2020.

[51] B. Sakthi, K. Durai, and J. Benadict Raja, “PSO-KNN BASED EFFECTIVE OPTIC DISC SEGMENTATION AND CLASSIFICATION IN FUNDUS IMAGES,” 2020.

[52] T. M. Khan, M. Mehmood, S. S. Naqvi, and M. F. U. Butt, “A region growing and local adaptive thresholding-based optic disc detection,” PLoS One, vol. 15, no. 1, Jan. 2020.

[53] V. Hayyolalam and A. A. Pourhaji Kazem, “Black Widow Optimization Algorithm: A novel meta-heuristic approach for solving engineering optimization problems,” Eng Appl Artif Intell, vol. 87, 2020.

[54] F. Shahabi, F. Poorahangaryan, S. A. Edalatpanah, and H. Beheshti, “A Multilevel Image Thresholding Approach Based on Crow Search Algorithm and Otsu Method,” Int J Comput Intell Appl, vol. 19, no. 2, 2020.

[55] Z. Xie, T. Ling, Y. Yang, R. Shu, and B. J. Liu, “Optic Disc and Cup Image Segmentation Utilizing Contour-Based Transformation and Sequence Labeling Networks,” J Med Syst, vol. 44, no. 5,2020.

[56] S. Singh, N. Mittal, and H. Singh, “A multilevel thresholding algorithm using LebTLBO for image segmentation,” Neural Computing and Applications, vol. 32, no. 21. Springer Science and Business Media Deutschland GmbH, pp. 16681–16706, Nov. 01, 2020.

[57] B. Chen *et al.*, “Abnormality detection in retinal image by individualized background learning,” Pattern Recognit, vol. 102, 2020.

[58] T. R. V. Bisneto, A. O. de Carvalho Filho, and D. M. V. Magalhães, “Generative adversarial network and texture features applied to automatic glaucoma detection,” Applied Soft Computing Journal, vol. 90,2020.

[59] A. Romero-Arellano *et al.*, “Image encryption and decryption system through a hybrid approach using the jigsaw transform and langton’s ant applied to retinal fundus images,” Axioms, vol. 10, no. 3, Sep. 2021.

[60] R. Praveena and T. R. GaneshBabu, “Determination of cup to disc ratio using unsupervised machine learning techniques for glaucoma detection,” MCB Molecular and Cellular Biomechanics, vol. 18, no. 2, pp. 69–86, 2021.

[61] R. Rimani, N. H. Said, A. Ali-Pacha, and J. A. L. Ramos, “An efficient image encryption using a dynamic, nonlinear and secret diffusion scheme,” Baghdad Science Journal, vol. 18, no. 3, pp. 628–639, 2021.

[62] R. Srikanth and K. Bikshalu, “Multilevel thresholding image segmentation based on energy curve with harmony Search Algorithm,” Ain Shams Engineering Journal, vol. 12, no. 1, pp. 1–20, 2021.

[63] M. Azad, M. Hasan, and M. K, “Color Image Processing in Digital Image,” International Journal of New Technology and Research, vol. 3, no. 3, 2017.

[64] J. Coady, A. O’Riordan, G. Dooly, T. Newe, and D. Toal, “An overview of popular digital image processing filtering operations,” in Proceedings of the International Conference on Sensing Technology, ICST, 2019.

[65] D. Puri, “COCO dataset stuff segmentation challenge,” in Proceedings - 2019 5th International Conference on Computing,” Communication Control and Automation, ICCUBEA 2019, 2019.

[66] A. Sharma, R. Chaturvedi, and A. Bhargava, “A novel opposition based improved firefly algorithm for multilevel image segmentation,” Multimed Tools Appl, vol. 81, no. 11, 2022.

[67] P. Upadhyay and J. K. Chhabra, “Kapur’s entropy based optimal multilevel image segmentation using Crow Search Algorithm,” Appl Soft Comput, vol. 97, 2020.

[68] V. Rajinikanth, N. Dey, E. Kavallieratou, and H. Lin, “Firefly Algorithm-Based Kapur’s Thresholding and Hough Transform to Extract Leukocyte Section from Hematological Images,” 2020.

[69] E. H. Houssein, B. E. din Helmy, D. Oliva, A. A. Elngar, and H. Shaban, “A novel Black Widow Optimization algorithm for multilevel thresholding image segmentation,” Expert Syst Appl, vol. 167, 2021.

[70] S. R. Gallagher, “Digital image processing and analysis with imagej,” Current Protocols in Essential Laboratory Techniques,2014.

[71] Z. Zhu, H. Chen, Y. Hu, and J. Li, “Age estimation algorithm of facial images based on multi-label sorting,” EURASIP J Image Video Process, vol. 2018, no. 1, 2018.

[72] H. Gao, Z. Fu, C. M. Pun, H. Hu, and R. Lan, “A multi-level thresholding image segmentation based on an improved artificial bee colony algorithm,” Computers and Electrical Engineering, vol. 70, 2018.

[73] P. Jyotiyana and S. Maheshwari, “Maximal Stable Extremal Region Extraction of MRI Tumor Images Using Successive Otsu Algorithm,” in Lecture Notes in Networks and Systems, 2019.

[74] N. B. Bahadure, A. K. Ray, and H. P. Thethi, “Image Analysis for MRI Based Brain Tumor Detection and Feature Extraction Using Biologically Inspired BWT and SVM,” Int J Biomed Imaging, 2017.

[75] M. Abd Elaziz, N. Nabil, R. Moghdani, A. A. Ewees, E. Cuevas, and S. Lu, “Multilevel thresholding image segmentation based on improved volleyball premier league algorithm using whale optimization algorithm,” Multimed Tools Appl, vol. 80, no. 8, 2021.

[76] S. B. Song, J. F. Liu, H. Y. Ni, X. lou Cao, H. Pu, and B. X. Huang, “A new automatic thresholding algorithm for unimodal gray-level distribution images by using the gray gradient information,” J Pet Sci Eng, vol. 190, 2020.

[77] M. Jin *et al.*, “An automatic detection method of solar radio burst based on Otsu binarization,” 2019.

[78] V. C. Test, S. Generation, and W. Afzal, “Swarm Intelligence - Volume 3: Applications,” Swarm Intelligence ,2018.

[79] H. S. Abdullah, “Comparative study of swarm intelligence behavior to solve optimization problems,” Engineering and Technology Journal, vol. 29, no. 14, 2011.

[80] T. Islam, M. E. Islam, and M. R. Ruhin, “An Analysis of Foraging and Echolocation Behavior of Swarm Intelligence Algorithms in Optimization: ACO, BCO and BA,” Int J Intell Sci, vol. 08, no. 01, pp. 1–27, 2018.

[81] G. Hu, B. Du, X. Wang, and G. Wei, “An enhanced black widow optimization algorithm for feature selection,” Knowl Based Syst, vol. 235, 2022.

[82] Y. Fu, Y. Hou, Z. Chen, X. Pu, K. Gao, and A. Sadollah, “Modelling and scheduling integration of distributed production and distribution problems via black widow optimization,” Swarm Evol Comput, vol. 68, 2022.

[83] V. Hayyolalam and A. A. Pourhaji Kazem, “Black Widow Optimization Algorithm: A novel meta-heuristic approach for solving engineering optimization problems,” Eng Appl Artif Intell, vol. 87, 2020.

[84] E. Korkmaz, “Energy demand estimation in Turkey according to modes of transportation: Bezier search differential evolution and black widow optimization algorithms-based model development and application,” Neural Comput Appl, 2023.

[85] V. Hayyolalam and A. A. Pourhaji Kazem, “Black Widow Optimization Algorithm: A novel meta-heuristic approach for solving engineering optimization problems,” Eng Appl Artif Intell, vol. 87, 2020.

[86] V. Hayyolalam and A. A. Pourhaji Kazem, “Black Widow Optimization Algorithm: A novel meta-heuristic approach for solving engineering optimization problems,” Eng Appl Artif Intell, vol. 87, Jan. 2020.

[87] N. A. Munirah, M. A. Remli, N. Mohd Ali, H. W. Nies, M. S. Mohamad, and K. N. S. W. Salihin Wong, “The Development of Parameter Estimation Method for Chinese Hamster Ovary Model using Black Widow Optimization Algorithm,” International Journal of Advanced Computer Science and Applications, vol. 11, no. 11, 2020.

[88] V. Hayyolalam and A. A. Pourhaji Kazem, “Black Widow Optimization Algorithm: A novel meta-heuristic approach for solving engineering optimization problems,” Eng Appl Artif Intell, vol. 87, 2020.

[89] A. M. R. Ibrahim ALattar, “A Comparative Study of Researches Based on Magic Square in Encryption with Proposing a New Technology,” IRAQI JOURNAL OF COMPUTERS, COMMUNICATIONS, CONTROL AND SYSTEMS ENGINEERING, vol. 21, no. 2, pp. 102–114, 2021.

[90] T.W. Khairi, “Framework For Modeling and Simulation of Secure Cloud Services,” Iraqi Journal of Computers, Communications, Control and Systems Engineering, vol. 22, no. 1, 2022.

[91] A. A. Zainab Muneef Hala bahjat, “Image Encryption Paillier Homomorphic Cryptosystem,” IRAQI JOURNAL OF COMPUTERS, COMMUNICATIONS, CONTROL AND SYSTEMS ENGINEERING, vol. 21, no. 4, pp. 29–36, 2021.

[92] Y. Kumar, R. Munjal, and H. Sharma, “Comparison of Symmetric and Asymmetric Cryptography with Existing Vulnerabilities and Countermeasures,” IJCSMS International Journal of Computer Science and Management Studies, 2011.

[93] F. Maqsood, M. Ahmed, M. Mumtaz, and M. Ali, “Cryptography: A Comparative Analysis for Modern Techniques,” International Journal of Advanced Computer Science and Applications, vol. 8, no. 6, 2017.

[94] S. Gautam, S. Singh, and H. Singh, “A Comparative Study and Analysis of Cryptographic Algorithms: RSA, DES, AES, BLOWFISH, 3-DES, and TWOFISH,” INTERNATIONAL JOURNAL OF RESEARCH IN ELECTRONICS AND COMPUTER ENGINEERING, vol. 7, no. 1, 2019.

[95] M. Harini, K. P. Gowri, C. Pavithra, and M. Pradhiba Selvarani, “COMPARATIVE STUDY AND ANALYSIS OF VARIOUS CRYPTOGRAPHIC ALGORITHMS,” Int J Sci Eng Res, vol. 8, no. 5, 2017.

[96] N. A. Wahid, A. Ali, B. Esparham, and M. Marwan, “A Comparison of Cryptographic Algorithms: DES, 3DES, AES, RSA and Blowfish for Guessing Attacks Prevention,” Journal of Computer Science Applications and Information Technology, vol. 3, no. 2, pp. 1–7, 2018.

[97] F. J. D’souza and D. Panchal, “Advanced encryption standard (AES) security enhancement using hybrid approach,” in Proceeding - IEEE International Conference on Computing, Communication and Automation, ICCCA , 2017.

[98] O. G. Abood and S. K. Guirguis, “A Survey on Cryptography Algorithms,” International Journal of Scientific and Research Publications (IJSRP), vol. 8, no. 7, 2018.

[99] U. Sara, M. Akter, and M. S. Uddin, “Image Quality Assessment through FSIM, SSIM, MSE and PSNR—A Comparative Study,” Journal of Computer and Communications, vol. 07, no. 03, 2019.

[100] X. Wang, S. Gao, L. Yu, Y. Sun, and H. Sun, “Chaotic image encryption algorithm based on bit-combination scrambling in decimal system and dynamic diffusion,” IEEE Access, vol. 7, 2019.

[101] A. A.-S. Hiba Yaseen, “Load Balancing and Detection of Distributed Denial of Service Attacks Using Entropy Detection,” IRAQI JOURNAL OF COMPUTERS, COMMUNICATIONS, CONTROL AND SYSTEMS ENGINEERING, vol. 21, no. 4, pp. 60–73, 2021.